

THE ADSORPTION OF FISSION PRODUCTS ON VHTR STRUCTURAL
MATERIALS

A Thesis presented to the Faculty of the Graduate School
at the University of Missouri-Columbia

In Partial Fulfillment
of the Requirements for the Degree
Doctor of Philosophy

by

SEAN BRANNEY

Dr. Tushar Ghosh, Thesis Supervisor

JULY 2010

The undersigned, appointed by the Dean of the Graduate School, have examined the thesis entitled

THE ADSORPTION OF FISSION PRODUCTS ON VHTR STRUCTURAL
MATERIALS

Presented by Sean Branney

A candidate for the degree of Doctor of Philosophy

And hereby certify that in their opinion it is worthy of acceptance.

Professor Tushar K Ghosh

Professor Sudarshan K Loyalka

Professor Mark A Prelas

Professor Robert V Tompson

Professor Dabir S Viswanath

ACKNOWLEDGMENTS

This thesis work would never have existed were it not for the support, financial and otherwise, of the faculty and staff of the Nuclear Science and Engineering Institute. They have my deepest gratitude and thanks for giving me this opportunity. I have been funded throughout my time at NSEI by GANN, NRC, DOE and NERI-C fellowships. I am very grateful for this support.

My thanks to my thesis advisor, Dr. Tushar Ghosh, who was always available and helpful whenever I needed to bounce one idea or other off him. His expertise and experience were invaluable in this project, and yet he still allowed me to pursue whichever path I thought to be most appropriate at each stage of this project.

I would like to thank Dr. Sudarshan Loyalka for his support throughout my time at the NSEI, without which I simply would not have gotten to this point. His expertise and thoroughly approachable demeanor make the NSEI the superb place that it is.

Dr. Mark Prelas introduced me to the field of non-proliferation, an area which has become one of my main interests in the field of nuclear engineering. For this, and

his expertise and willingness to share some of his experiences in the area, he has my sincere thanks.

The oft heard battle cry of Dr. Tompson, "Get back to work!" was extremely motivational.

The ability of Dr. Viswanath to find any piece of literature anywhere was extremely valuable to me. One might speculate that there are some journals published and distributed only to him, such is the elusiveness of some of the things he is able to find.

I would like to thank James Bennett of the NSEI who always ensured, no matter what, we were getting paid in the end. Latricia Vaughan was always very helpful and understanding of the fact that, while I may eventually finish a Ph.D in Nuclear Engineering, I certainly was not capable of filling out the correct forms along the way without a lot of assistance.

Sam Potts of the physics machine shop did a lot of work in support of this thesis, without which many of the things we did would simply not have been possible.

Dr. Mike Glascock was helpful in analyzing my iodine samples using NAA. I appreciate his help.

Jim Guthrie's ICP analysis was vital in acquiring much of the data we needed.

Sorry I broke your machine by choking it with cesium, Jim.

I would like to thank my parents for their constant support throughout my life which has never decreased with my age, nor my now considerable distance from home. More than anything, I am grateful that because of them I know that no matter how far you go from it, home will always be home.

My in-laws, Russel and Judy Ellis, utterly mock the in-law stereotype by being superb people who have supported me ever since I came to the United States. Their continued support has greatly assisted in any success I have had since coming to the United States.

I would like to thank my brother, Ciaran. Nothing motivates a man to finish his Ph.D like his younger brother getting one before him. Keep working on those engines. Nothing on earth sounds like twenty Formula 1 cars arriving at the first corner, all screaming at 20,000 rpm. The world is a better place for it.

Thomas Boyle's knowledge of Mathematica was extremely useful to me. Much of my data analysis owes itself to his abilities to make something of my snarling, "It doesn't work, fix it!". My powerlifting total owes a lot to my competing with his, also.

Ray Maynard leaned over on the first day of Radiation Biology way back in 2004 when I first started my Masters studies and said, "So, why are you here?". His comradeship ever since has been very valuable to me.

Jason Wilson taught me that you can tell a bolt is tight enough when all your strength can't make it turn anymore. You can say many things about my setup, but there were no leaks in it!

I would like to thank all the other students who have come and gone from NSEI in my time here. Special thanks to Lynn Tipton and Zebidiah Smith for showing us it is possible to eventually finish! My thanks to Kyle Walton, also, for the isotherm classification diagram.

I would also like to thank some friends from back home for staying in touch through all these years. Christopher Brannigan, Keith Goddard, John Hinds and Gerald Mc Alister.

Finally, I would like to thank my lovely wife, Robin. Without her constant support and help, the inevitable slide into madness would have been much more rapid.

To everyone who has helped me up to this point, go raibh mile maith agaibh. Adh mór ort.

TABLE OF CONTENTS

ACKNOWLEDGMENTS	ii
LIST OF FIGURES	ix
LIST OF TABLES	xiii
ABSTRACT	xiv
Chapter 1 - Introduction	1
1.1 - Introduction	1
Chapter 2 - Theory	7
2.1 – Vapor Pressure	7
2.2 – Adsorption Theory	11
2.3 - Heats of adsorption.....	19
Chapter 3 - Literature Review	24
3.1- Vapor pressure data	24
3.2 – Adsorption literature	39
3.3 – Analysis of GA data for cesium adsorbed on graphite	43

Chapter 4 - Experimental Design.....	51
4.1 – Introduction	51
4.2 – Analysis methods.....	53
4.2.1 – Thermo gravimetric Analyzer	53
4.2.2 – Neutron Activation Analysis	58
4.2.3 – Inductively Coupled Plasma Mass Spectroscopy.....	59
4.2.4 – Energy Dispersive Spectroscopy	62
4.3 –Experimental Setups.....	64
4.3.1 – Setup for initial testing.....	64
4.3.2 – TGA Setup	65
4.3.3 – Cesium cell and column setup	69
Chapter 5 - Results and Discussion	76
5.1 – Initial scoping experiment with cesium iodide	76
5.2 – Iodine experiments.....	81
5.3 – ICP analysis of cesium adsorbed on graphite in TGA.....	84
5.4 – ICP analysis of cesium adsorbed on graphite using cesium cell and inconel columns	87
Chapter 6 - Conclusion.....	94
BIBLIOGRAPHY.....	98

VITA 103

LIST OF FIGURES

Figure 1 - Diagram of Prismatic VHTR core	4
Figure 2.1 - Typical Langmuir Isotherm	16
Figure 2.2 - Typical BET Isotherm	17
Figure 2.3 – Eight types of isotherm as characterized by Brunauer and Jonvanovic. Type 1 is a typical Langmuir isotherm usually indicative of simple physisorption. Type 2 is a BET isotherm. Type 3 is a classical chemisorption isotherm. Later isotherm types show more complex adsorption behavior with the exception of type 7 which is a simple Henrian isotherm.	18
Figure 3.1.1 – Combined plot of cesium vapor pressure literature data	26
Figure 3.1.2 – Three different fits to the literature cesium vapor pressure data ..	28
Figure 3.1.3 – Clausius-Clapeyron fit for cesium literature data	29
Figure 3.1.4 – Antoine fit to cesium literature data	30
Figure 3.1.5 – Reidel fit to cesium literature data	31
Figure 3.1.6 - Three different fits to the literature iodine vapor pressure data	32
Figure 3.1.7 - Three different fits to the literature strontium vapor pressure data	33
Figure 3.1.8 - Three different fits to the literature silver vapor pressure data	34

Figure 3.1.9 - Three different fits to the literature palladium vapor pressure data	35
Figure 3.3.1 – Adsorption data for cesium on graphite as reported by General Atomic	45
Figure 3.3.2 – Plot of isotherm calculation for different loadings of cesium on graphite from GA data	46
Figure 3.3.3 – Variation of heat of adsorption as loading increases. The approach to the heat of condensation is clearly discernable	48
Figure 3.3.4 - GA data with Langmuir (solid colour lines) and IAEA (dashed lined) fits	49
Figure 4.2.1 – Schematic diagram of the balance component for the TGA system reproduced from Thermofisher’s TGA manual	55
Figure 4.2.2 – Complete TGA system	56
Figure 4.2.3 – Diagram of typical ICP-MS system from http://www2.fiu.edu/~almirall/Lecture19.pdf	61
Figure 4.3.1 - Initial testing setup	64
Figure 4.3.2 – TGA system setup schematic	66
Figure 4.3.3 – TGA system	66
Figure 4.3.4 – Cesium vapor production cell used in this study	71

Figure 4.3.5 – Experimental setup including cesium cell, splitting manifold and sample columns.....	75
Figure 5.1.1 – EDS image of stainless steel strip exposed to cesium iodide vapor. The spheres coating the surface were analysed and found to be composed entirely of cesium iodide	77
Figure 5.1.2 – A close up image of one of some of the spheres from the previous figure. A small hole is evident in the sphere in the lower right. This was the result of the electron beam being used to analyze its composition	78
Figure 5.1.3 – EDS spectrum of the sphere from the previous figure. Elemental analysis shows the sphere is composed almost entirely of cesium and iodine...	79
Figure 5.1.4 – EDS spectrm of the bulk material surrounding the spheres in figure 5.1.2. The spectrum shows no cesium or iodine present indicating that the cesium and iodine detected in the spheres were, as expected, not part of the bulk material	80
Figure 5.2.1 – Gamma spectrum from NAA on graphite samples with adsorbed iodine.....	83
Figure 5.3.1 – Results of ICP analysis of graphite samples with adsorbed cesium	86
Figure 5.4.1 – Data from the ICP analysis of samples with cesium adsorbed on graphite	92

Figure 5.4.2 - Data from the ICP analysis of samples with cesium adsorbed on
graphite with range closer to the origin 93

Figure 6.1 – Possible future graphite sample arrangement 96

LIST OF TABLES

Table 3.1 – Constant values and average error for literature cesium data fits....	27
Table 3.2 - Constant values and average error for literature iodine data fits	36
Table 3.3 - Constant values and average error for literature strontium data fits .	36
Table 3.4 - Constant values and average error for literature silver data fits	37
Table 3.5 - Constant values and average error for literature palladium data fits	37
Table 3.6 - A summary of the literature on the adsorption of fission products on structural materials of interest in VHTRs.	39
Table 5.1 – Results of NAA for iodine adsorbed on graphite for varying lengths of time.....	82
Table 5.2 – Adsorbed amounts of cesium on graphite samples from ICP analysis	88

ABSTRACT

The Very High Temperature Reactor (VHTR) is being considered as a candidate for the next generation of nuclear reactors. There are several areas that require further study in VHTR reactor designs. One such area is the adsorption of fission products on the reactor's structural materials, such as graphite and stainless steel. It is important to know how much of these fission products have adsorbed on various parts of the reactor both for the purposes of understanding the possible activity of the components during maintenance operations, and also to quantify potential releases of these fission products during accident scenarios. The adsorption of fission products on reactor materials has been studied in the past, but further data are required, particularly data describing adsorption at the extremely low vapor pressures of fission products that may be present in a VHTR core.

This project was undertaken in order to acquire some of these data. Several experimental systems were designed and built throughout the course of this project, with a final design using a specially designed cell to produce cesium vapor and a series of inconel columns containing graphite samples. Several

analysis methods were used during the course of this study, including Gravimetry, Neutron Activation Analysis, Energy Dispersive Spectroscopy, and Inductively Coupled Plasma Mass Spectroscopy. NAA and ICP were found to be the methods best suited to our analysis needs.

Some isotherm data has been generated and recommendations for future work have been formulated.

Chapter 1 - Introduction

1.1 - Introduction

The Generation IV International Forum (GIF) is an international consortium of ten international government entities that are working together to develop next generation (Gen IV) nuclear energy systems to meet the world's future energy needs while reducing carbon emissions into the atmosphere. The GIF has selected six designs of nuclear energy systems. However, each participating country is allowed to choose its own system. The Very High Temperature Reactor (VHTR) is one such system that the US has adopted for further study, leading to commercial development. Two types of designs have been proposed, the prismatic design and the Pebble Bed Modular Reactor (PBMR). The VHTR design has several advantages over the current conventional Light Water Reactors (LWR's). LWRs are limited in their thermal efficiency by the physical properties of their moderator and coolant, water. The thermodynamic efficiency of a plant is limited by the outlet coolant temperature; the higher the temperature, the higher the possible efficiency. However, the materials used in construction of steam turbine tubes and other parts of the plant that can withstand high temperature steam at supercritical conditions limit the efficiency of LWR power plants. VHTRs use gaseous coolants (generally helium) that allow much higher

outlet temperatures. Gaseous coolants also have the advantage of avoiding a phase change in the cooling cycle. Using water as a coolant, even in a PWR, the liquid coolant is converted to steam in the steam generator and is later condensed after it drives the turbine. This phase change can be problematic for several reasons. The main issue that occurs relating to this phase change during normal operation is the formation of small droplets of water in the steam driving the turbine. These droplets impact on the turbine blades and cause pitting. A phase change is also a serious issue during an accident, since if the temperature increases and causes the coolant to boil; the steam produced is much less efficient at removing heat from the core than pressurized liquid water.

The use of helium as a coolant allows for outlet temperatures approaching 1000 °C. A thermal efficiency of close to 50% (45-48%) is achievable with these reactor designs. Helium also does not absorb neutrons, unlike water. This means that the reactor coolant remains much less radioactive than the coolant loop in a LWR. However, the fission products can still escape from the VHTR fuel system and contaminate various parts of the plant, including the gas turbine. In this research project, the focus is on PBMR systems and is discussed further below.

PBMR's use a type of coated particle known as a TRISO (Tri-isotropic) particle as fuel. The sizes of these particles and the thicknesses of the layers composing them vary from fuel design to fuel design, but they all share a common design concept. At the center of each TRISO particle is a kernel of fissile material

(Uranium dioxide, Uranium carbide and Uranium oxycarbide have all been used). This fissile material is surrounded by a layer of porous graphite. The purpose of this layer is to absorb fission products as they are produced by fission in the fissile center and to allow for mechanical deformations of the particle. Outside this layer is a layer of pyrolytic graphite and silicon carbide. This layer forms a barrier to the transport of fission products outside the fuel particle. The final layer of the fuel particle is another layer of pyrolytic graphite the purpose of which is to protect the particle. Some 15,000 of these particles are then embedded in a sphere of graphite matrix forming the fuel pebbles that give this reactor type its name.

The PBMR design uses approximately 450,000 of these pebbles in the core at a time. One of the main advantages of the PBMR design is this fuel form. The reactor core is a vessel containing these fuel pebbles, with helium gas flowing through as coolant. During the course of operation, the pebbles move through the core and some are ejected at the bottom of the core. These pebbles are then inspected for defects, and if none are found, are reinserted into the top of the core, all while the reactor is online and operating. On its own, this is a huge advantage to the PBMR design. Like the Canadian CANDU reactors, the PBMR can be refueled online, eliminating the need to shut down during refueling, and increasing the capacity factor of the reactor significantly.

Prismatic VHTR's also use TRISO particles, but instead of being embedded in graphite spheres, as in the PBMR, the particles are embedded in a large graphite column. This being the case, the TRISO particles do not move around as they do in a PBMR. The graphite column is sectional, and vertical sections of the column can be removed individually for refueling and maintenance.

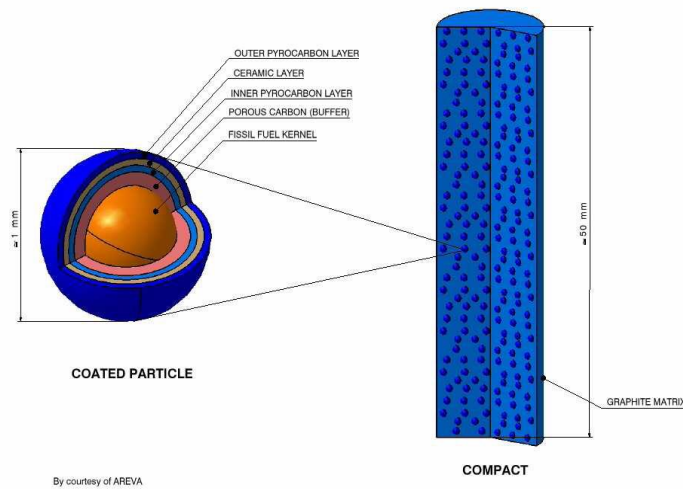


Figure 1 - Diagram of Prismatic VHTR core

While the TRISO fuel particles are engineered to prevent the leakage of fission products, mechanical defects that occur during manufacturing or that develop during operation can lead to some release of these fission products into the reactor's coolant. It is important to account for these fission products after they escape the fuel particle. Some quantity of the escaped fission products will adsorb on the graphite in the reactor core, both on other fuel pebbles and on other graphite core components (such as the spire in a PBMR, or the prismatic blocks of a prismatic reactor) of the core. Fission products not retained in the

core may then be adsorbed on other structural components of the reactor system including the coolant heat exchanger and the turbine. To allow for the safe maintenance of the reactor, it is crucial to know what the activities of the various components of the reactor may be at any time as a result of fission product adsorption. This issue becomes even more critical in the event of an accident when a large temperature rise may result in the release of these fission products.

The goal of this research is to acquire data and develop a model, as needed, to explain the adsorption behavior of some fission products of interest. The fission products of interest are iodine, cesium, strontium, palladium and silver. The first three of these elements have isotopes that are important in reactor design considerations because of their health effects. Cesium is chemically similar to sodium, and can form many compounds analogous to their sodium counter parts and can therefore be metabolized. Strontium has a similar relationship to calcium. Iodine is a compound that concentrates in the thyroid gland, and so is of interest in terms of its health effects. Silver and Palladium are mainly of interest because of their effects on the structure of VHTR fuel particles. It is thought that their diffusion from the fissile core of TRISO fuel particles may damage the fuel in such a way as to make further release of fission products more likely.

An extensive review of the literature indicated the lack of adequate adsorption data for these fission products on structural materials of interest in VHTRs. The

existing data from various researchers are also inconsistent and there is a lack of data on current structural materials at temperatures up to 1000°C.

Chapter 2 - Theory

2.1 - Vapor Pressure

All substances have a distribution of molecular (or atomic) velocities usually described by a Maxwellian distribution. In order for a phase change to occur, an atom or molecule must acquire enough energy to break the bonding that holds it in its current state. In the case of a solid, these will generally be covalent, ionic, or metallic bonds. It follows, then, that given an energy distribution in a substance in any phase, some of the atoms or molecules will possess the amount of energy needed to move into another phase. This is why a droplet of water left on a surface at room temperature will eventually evaporate, despite the fact that its temperature is far below its boiling point.

While some atoms or molecules will evaporate in this manner, other atoms or molecules from the vapor phase will themselves condense. The rate at which both of these processes happen will depend on the energy distribution of the atoms or molecules, which is equivalent to their temperature. At a given temperature in a closed system, evaporation will occur at a certain rate and condensation will occur at a certain rate. The magnitudes of these two rates will determine an equilibrium concentration in the vapor phase. This is the origin of

vapor pressure. For a given substance in a closed system, there will be a constant vapor pressure above the substance depending on the temperature of the system. As previously stated, it is the vapor pressure that allows liquids to evaporate below their boiling point, but even solids do, theoretically, have a small vapor pressure above them.

The precise dependence of the vapor pressure of a substance on temperature varies from substance to substance. It is a function of a number of parameters, including the strength and type of bonding present, and the molecular weight of the substance.

A relationship between vapor pressure and temperature can be derived from thermodynamic considerations²³. We begin with one of Maxwell's relations:

$$\left(\frac{\partial p}{\partial T}\right)_V = \left(\frac{\partial S}{\partial V}\right)_T \quad (2.1.1)$$

We are interested in the vapor pressure at a constant T. We can therefore write 2.1.1 as

$$\left(\frac{\partial p}{\partial T}\right)_V = \left(\frac{\Delta S}{\Delta V}\right) \quad (2.1.2)$$

Since

$$\Delta S = \frac{\Delta H}{T} \quad (2.1.3)$$

and the volume of the gaseous phase is much larger than the liquid phase

$$\Delta V = V_{gas} - V_{solid\ or\ liquid} \approx V_{gas} \quad (2.1.4)$$

2.1.2 then becomes

$$\frac{dp}{dT} = \frac{\Delta H}{T(V_g)} \quad (2.1.5)$$

Secondly, we will assume that the gas species is ideal such that the ideal gas law applies.

$$V = \frac{nRT}{p} \quad (2.1.6)$$

Where n is the number of moles of gas present and R is the gas constant. This gives us

$$\frac{dp}{dT} = \frac{\Delta H' p}{RT^2} \quad (2.1.7)$$

Where $\Delta H'$ is the enthalpy per mol. This is known as the Clausius-Clapeyron equation. Rearranging, we obtain

$$\frac{dp}{p} = \frac{\Delta H'}{R} \frac{dT}{T^2} \quad (2.1.8)$$

Finally, integrating this equation gives us

$$\ln(p) = \frac{\Delta H'}{RT} + c \quad (2.1.9)$$

Which we can write in the form

$$\ln(p) = A + \frac{B}{T} \quad (2.1.10)$$

Equation 2.1.15 gives us a simple relation between the vapor pressure of a species and its temperature. The assumptions involved in its derivation mean that different species will follow this relation to differing extents, particularly depending on how valid the ideal gas assumption is for that species.

Other models have been developed to try to better account for the vapor pressure of real species. One such model is the Antoine equation

$$\ln(p) = A - \frac{B}{C+T} \quad (2.1.11)$$

Another is the Reidel equation

$$\ln(p_R) = A - \frac{B}{T_R} + C \ln(T_R) + DT_R^6 \quad (2.1.12)$$

where p_R and T_R are the reduced pressure and temperature respectively.

As might be expected, models including more terms can often more accurately predict the vapor pressures of real species as temperatures vary.

2.2 – Adsorption Theory

Adsorption is a process by which a fluid or vapor adheres to a solid surface, forming layers. It arises in a manner similar to that which produces surface tension in liquids. At the surface of a solid, the outermost atoms are not bound to the same number of adjacent atoms as they would be in the bulk of the material since there are no further atoms in the direction normal to the surface. This produces a site where an adsorbate may approach and adhere.

Adsorption generally takes one of two forms, physisorption or chemisorption. Physisorption is a result of the surface atoms of an adsorbent interacting with the gas phase atoms of an adsorbate through either weak Van der Waals force, columbic force or hydrogen bonding. Because of the weak nature of these forces, physisorption is generally a low temperature phenomenon. As a result of this, the lower the temperature, the higher is the amount adsorbed. In addition, either by increasing the system temperature or lowering the pressure of the adsorbate, the adsorbate could be desorbed from the adsorbent surface.

Chemisorption occurs when surface atoms in the adsorbent chemically bond with atoms of the adsorbate. Chemisorption generally takes place at higher temperatures as a result of this and generally is not reversible merely by decreasing the temperature or pressure of the adsorbent-adsorbate system

In general, chemisorption has a higher heat of adsorption than physisorption. This is a result of the stronger bonds formed during chemisorptions. Calculation of the heat of adsorption can then be used in many cases to distinguish between chemi and physisorption.

There are several different models describing adsorption processes that attempt to account for the phenomena under different conditions. Part of the goal of this research is to attempt to establish which model best describes the adsorption of these fission products on VHTR structural materials.

The three most common models of adsorption are those of Freundlich, Langmuir and the BET model. The Freundlich isotherm is an attempt to account for adsorption processes in a purely empirical fashion. It can be represented by the following general equation²⁴:

$$a = \alpha p^{\frac{1}{n}} \quad (2.2.1)$$

Where 'a' is the amount adsorbed per unit weight of the adsorbent, 'p' is the pressure of the adsorbate and 'α' and 'n' are both constants. This isotherm is somewhat adequate for moderate pressures of adsorbate under certain conditions, but does not account well for adsorption behavior at high or low pressures. At very low pressures with a weakly adsorbing gas, the constant n is generally equal to one and the adsorption process obeys Henry's law with the amount adsorbed being proportional to the concentration of the adsorbate. In

general, this type of isotherm is more useful in describing the adsorption of solutions than the adsorption of gases.

Langmuir attempted to derive an isotherm by considering molecular kinetics. He considered adsorption as an equilibrium process with competing rates of condensation onto and evaporation from the surface. The rate of condensation on the surface will be proportional to $(1-\Theta)$ where Θ is the fractional coverage of the surface by the adsorbate and the rate of evaporation is proportional to Θ^{25} . His model is based on the following assumptions. Adsorption proceeds until the formation of a monolayer of adsorbate, and, the adsorbed molecules do not interact with each other on the surface they are adsorbed on. Langmuir states that while adsorbate molecules do condense on other adsorbed molecules, they evaporate much faster, effectively leaving only a monolayer on the surface. The surface is uniform; no site is more favorable to adsorption than any other. Finally, the adsorption mechanism is the same for all molecules adsorbed. The first molecule adsorbed on the surface is adsorbed in the same manner as the last molecule adsorbed, and the mechanism does not take into account multilayer adsorption.

Langmuir's model takes the following general form²⁴:

$$a = \frac{\kappa\lambda\mu}{1+\kappa\mu} \quad (2.2.2)$$

Where a is again the amount adsorbed per unit weight of the adsorbent, κ and λ are constants and μ is the pressure of the adsorbate.

The Langmuir model is best suited for type I isotherms, a typical Langmuir isotherm is shown in figure 2.1.

Recognizing that monolayer formation does not account for adsorption processes in all circumstances, Brauner, Emmett and Teller developed a model to take into account multilayer adsorption. The general equation of the BET model is as follows²⁶:

$$v = \frac{v_m c p}{(p_0 - p) \{1 + (c-1) (p/p_0)\}} \quad (2.2.3)$$

where v is the volume absorbed, v_m is the volume of the surface available for adsorption, c is a constant, p is the pressure of the adsorbate and p_0 is the saturation pressure of the adsorbate. BET isotherms have a characteristic 'S' shape, the first part of which is very similar to a Langmuir isotherm while a first monolayer forms. In the regime where p is much less than p_0 , and noting that in general the value of c is much larger than one, this equation reduces to the following special form of the Langmuir equation:

$$v = \frac{\left(\frac{v_m c}{p_0} p\right)}{\left(1 + \frac{c}{p_0} p\right)} \quad (2.4)$$

The BET model assumes that subsequent layers can form on top of the initial monolayer but does not require that additional complete layers form before a

further layer can begin to form on top of a partial layer. A typical isotherm that could be correlated best by the BET model is shown in figure 2.2.

There are several other common forms of isotherms that generally arise under conditions where some of the assumptions of Langmuir or BET theory are not true. For example, in a system where adsorbed molecules do interact with each other on the adsorbent surface, the adsorption isotherm will be different.

Brunauer and later Jovanovic classified a total of eight types of adsorption isotherms. Figure 2.3 shows these eight isotherm types.

Each of these isotherm models are valid in specific cases, with the BET isotherm perhaps being the most generally applicable. The experiments being proposed here are all performed at high temperatures where we expect chemisorption to be the dominant mechanism.

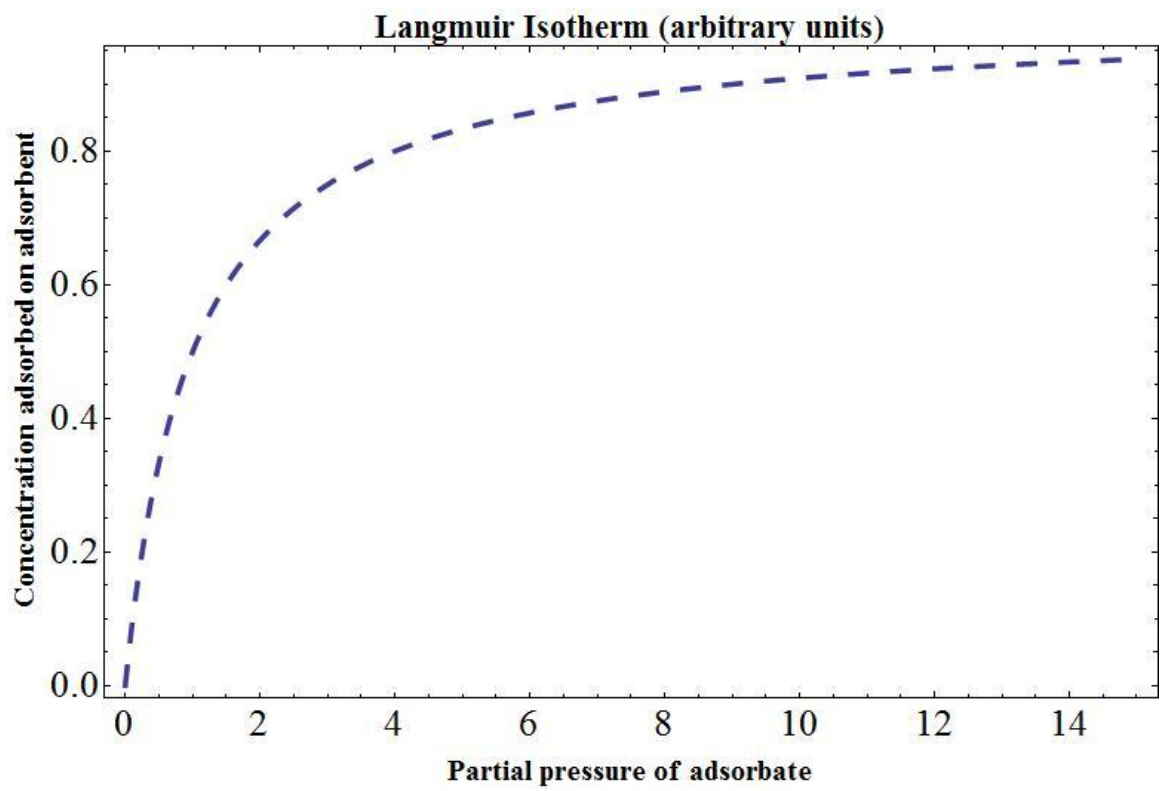


Figure 2.1 - Typical Langmuir Isotherm

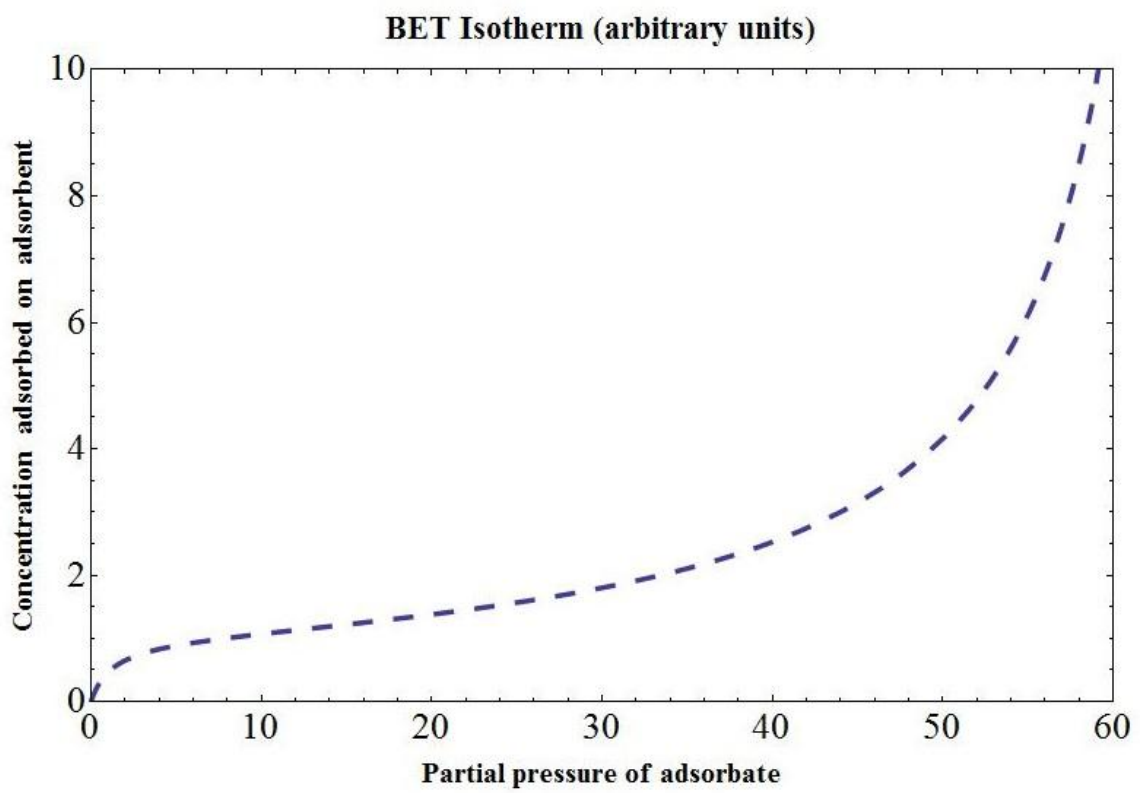


Figure 2.2 - Typical BET Isotherm

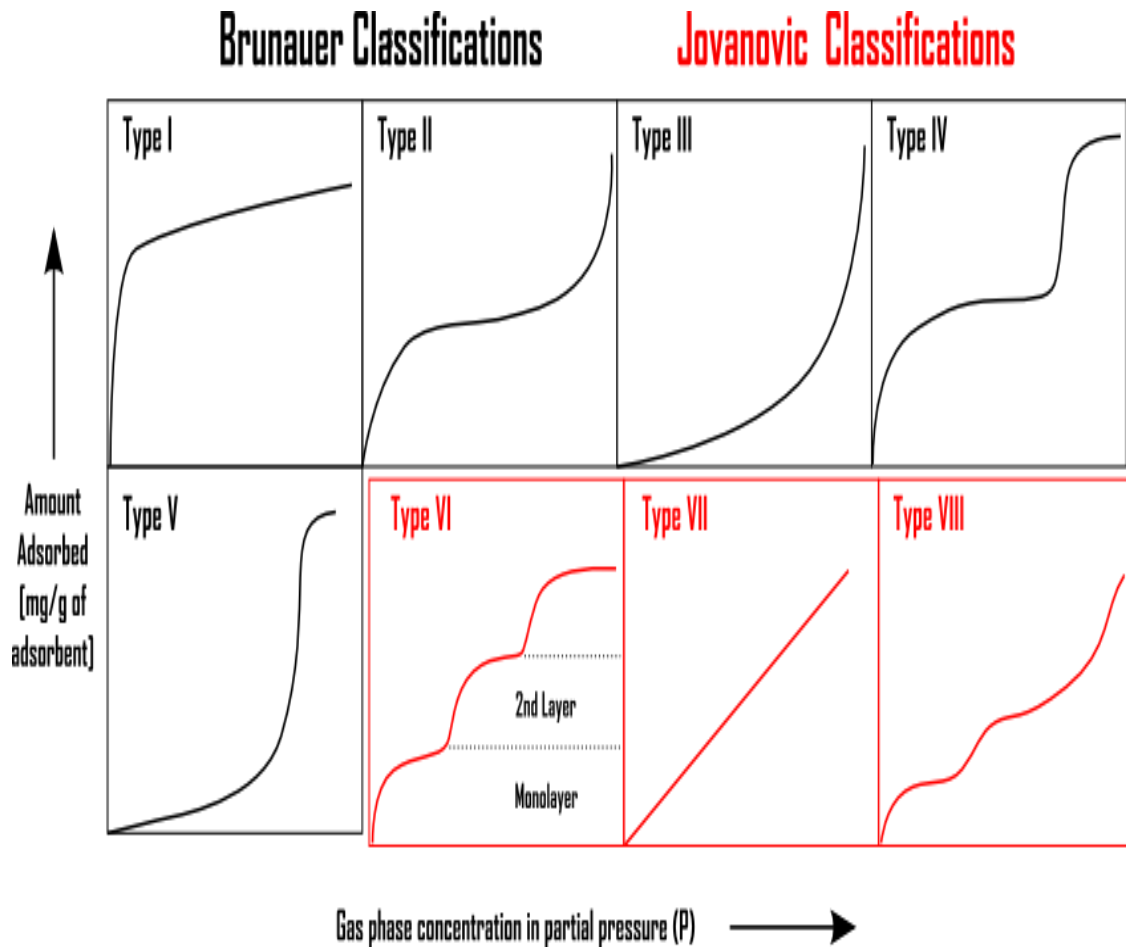


Figure 2.3 – Eight types of isotherm as characterized by Brunauer and Jonvanovic. Type 1 is a typical Langmuir isotherm usually indicative of simple physisorption. Type 2 is a BET isotherm. Type 3 is a classical chemisorption isotherm. Later isotherm types show more complex adsorption behavior with the exception of type 7 which is a simple Henrian isotherm.

2.3 - Heats of adsorption

As we have previously stated, it is useful to distinguish between chemisorptions and physisorption for the purposes of estimating how much of the adsorbed fission products may desorb in the event of an accident. In theory, fission products that are held weakly to the adsorbents we are studying by physisorption type potentials may rather easily desorb in an accident scenario whereas, chemisorbed fission products should be more strongly bonded to the adsorbent and may not desorb under the same conditions.

One method distinguishing between the two adsorption types is to calculate the heat of adsorption for the adsorption process taking place. The heat of adsorption is the amount of energy released when an adsorbate atom or molecule adsorbs on the adsorbent. The magnitude of this energy release is indicative of the strength of the bond formed during the adsorption event. The higher the energy release, the stronger the bond and the more likely the adsorption event was a chemisorption.

There are several methods of calculating the heat of adsorption depending on the conditions of the system where the measurement is being taken. If the temperature of the system is held constant while the heat of adsorption is measured, for example, by using a temperature bath, then the calculated heat of adsorption will be an isothermal heat of adsorption. If the measurement is taken

in a closed system where a moveable piston will allow the system pressure to remain constant during the adsorption process, the measured heat of adsorption in this case will be the isobaric heat of adsorption.

In general, we can define a heat of adsorption 'q' such that

$$q = \frac{dQ}{dn_s} \quad (2.3.1)$$

Where dQ is the amount of heat transferred to the surroundings and dn_s is the number of moles of gas adsorbed in the process ²⁷.

The total amount of heat adsorbed in the process will then be

$$Q = \int_0^{n_s} q dn_s \quad (2.3.2)$$

Assuming the chamber where the adsorption measurement is taken is inert and that the adsorbent is also inert (which may be more or less accurate, depending on the particular adsorbent) we can say

$$dQ = -dE - pdV \quad (2.3.3)$$

Where E will be the total energy of the gas and adsorbent, p is the system pressure and V will be the combined volume of the gas and adsorbate.

If we examine an adsorption process during which neither the volumes of the gas and adsorbent do not change nor does the surface area of the adsorbent 2.3.3 becomes

$$dQ_{V_G, V_S, A} = -dE_G - dE_S \quad (2.3.4)$$

Since dn_s is the number of moles adsorbed on the adsorbent and so, leaving the gas phase we can write

$$dn_G = -dn_S \quad (2.3.5)$$

We define E'_G as

$$E_G = n_G E'_G \quad (2.3.6)$$

Using equation 2.3.3 we can then define a quantity referred to as the differential heat of adsorption as

$$q_{V_G, V_S, A} = E'_G - \left(\frac{\partial E_S}{\partial n_S} \right)_{V_S, A, T} \quad (2.3.7)$$

If we consider a system that is also isobaric in addition to being isothermal, we can rewrite 2.3.3 as

$$dQ_{p, A, T} = -dE_G - dE_S - p dV_G - p dV_S \quad (2.3.8)$$

It can be shown that

$$dE_S = T dS_S - P dV_S - \phi dA - \mu_S dn_S \quad (2.3.9)$$

Where S is the entropy, ϕ is defined as $-\left(\frac{\partial E_S}{\partial A} \right)_{S_S, V_S, n_S}$ and ' μ ' is the chemical potential.

Substituting, we obtain

$$dQ_{p,A,T} = -d(E_G + pV_G) - TdS_S - \mu_S dn_S \quad (2.3.10)$$

The enthalpy of the system, H , is equal to $E+pV$. In a similar fashion to our definition of E' from equation 2.3.6 we can define

$$H = H' dn_S \quad (2.3.11)$$

and

$$S'_S = \left(\frac{\partial S_S}{\partial n_S} \right)_{P,T,A} \quad (2.3.12)$$

Rewriting equation 2.3.10 gives

$$dQ_{p,A,T} = H'_G dn_S - TS'_S dn_S - \mu_S dn_S \quad (2.3.13)$$

At equilibrium, the chemical potentials of the surface and gas will be equal; we can say the following

$$\mu_S = \mu_G = H'_G - TS'_G \quad (2.3.14)$$

Using equations 2.3.1 and 2.3.13 then gives us

$$q_{p,A,T} = TS_G - TS'_S \quad (2.3.15)$$

For an ideal gas as the adsorbate, it can be shown that at a constant loading of the adsorbent, n_S

$$\left(\frac{\partial}{\partial T} \ln(p) \right)_{n_S,A} = \frac{S_G - S'_G}{RT} \quad (2.3.16)$$

Noting this, equation 2.3.15 can be rewritten as a heat of adsorption at constant loading

$$q_{st} = -R \left(\frac{\partial}{\partial \frac{1}{T}} \ln(p) \right) \quad (2.3.17)$$

This particular heat of adsorption, the isotheric heat of adsorption, in this form will be a convenient method of calculating heats of adsorption for our experiments and will allow us to make some determination of whether we are observing chemisorption or physisorption.

Chapter 3 - Literature Review

3.1- Vapor pressure data

The experimental systems that have been designed during this project all require samples of VHTR structural materials be exposed to low concentrations of fission products suspended in a gas stream. Because of the variety of fission products these systems have been constructed to produce, it is difficult to make real time measurements of the fission product concentration present in the gas stream the samples are being exposed to. A system designed to make real time measurements of iodine concentration, for example, a PID detector, is unlikely to be suitable for the detection of cesium or strontium. It is necessary, then, to have an indirect method of determining the concentrations of each fission product we wish to study.

In the previous chapter we have described how the vapor pressure of a substance might vary with temperature, and given some models for making such predictions. Temperature being vastly simpler to measure than fission product concentration, it was necessary for us to gather as much data as possible relating

to the vapor pressures of these fission products so that we may calculate their concentrations from the temperatures we are exposing them to.

The vapor pressures of many elements have been extensively studied for many years, although some of the fission products of interest to us have not been extensively studied. There is a large body of literature on the vapor pressure of cesium^{1,2,3,4,5}, iodine^{6,7,8,9,10} and strontium^{11,12,13,14,15} with less data being available for silver^{18,19,20,21,22} and palladium^{16,17,18}. With their much higher boiling points, the vapor pressures of silver and palladium are significantly more difficult to measure than the other fission products in this study.

Vapor pressure measurements have been performed in many different ways by different experimenters and it is not the intention here to give an exhaustive analysis of the various methods used. Data was acquired from a large number of sources and combined in order to best fit the data over the widest possible temperature range. No attempt was made to test the validity of any particular method except in so far as all the data used in our fitting were shown to be consistent with each other.

For each fission product, all the available data from each source was combined into a single set of data. Fits were then calculated for this combined set using the Clausius-Clapeyron equation, the Antonie equation and the Reidel equation.

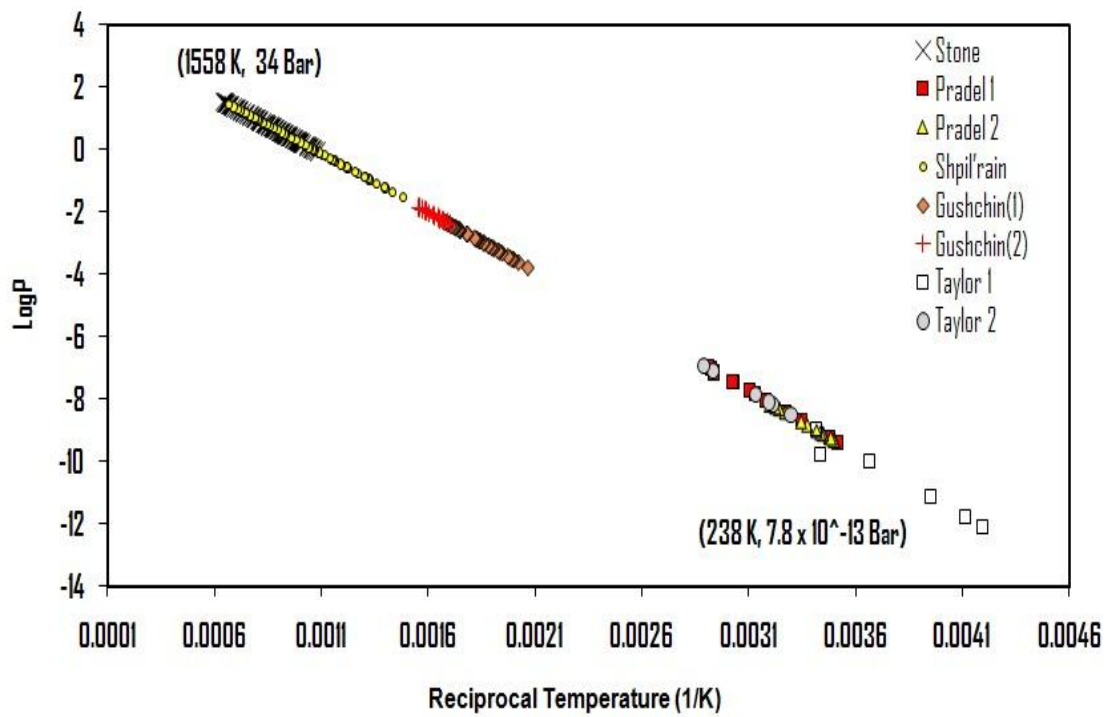


Figure 3.1.1 – Combined plot of cesium vapor pressure literature data

Figure 3.1.1 shows the literature data for cesium. All the sources appear to be consistent with each other and the relationship appears to be approximately linear. Figure 3.1.2 shows each of the three fits and the original data for cesium combined. Figure 3.1.3 shows the Clausis-Clapeyron fit to the literature data for cesium. Figure 3.1.4 is the Antoine fit to the cesium data and figure 3.1.5 is the Reidel fit. Table 3.1 shows the value of the constants in each fit and the average error for the entire data set using each fit.

Table 3.1 – Constant values and average error for literature cesium data fits

	A	B	C	D	Average error %
Clausis-Clapeyron	4.03775	3806.9	NA	NA	5.02
Antoine	3.8689	3590.22	-13.9782	NA	2.30
Reidel	3.99898	2.07189	-0.37336	0.133906	1.18

It is clear that in this case, the Reidel equation most accurately predicts the vapor pressure of cesium.

The combined fit plots and tables of constants and error for the other four fission products are shown below.

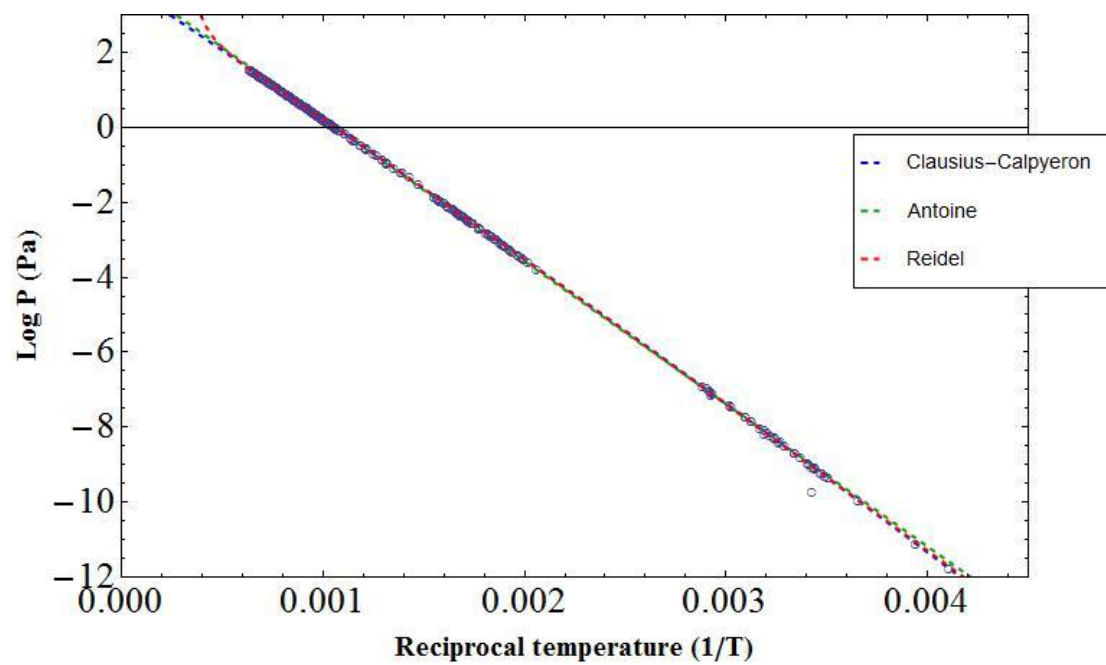


Figure 3.1.2 – Three different fits to the literature cesium vapor pressure data

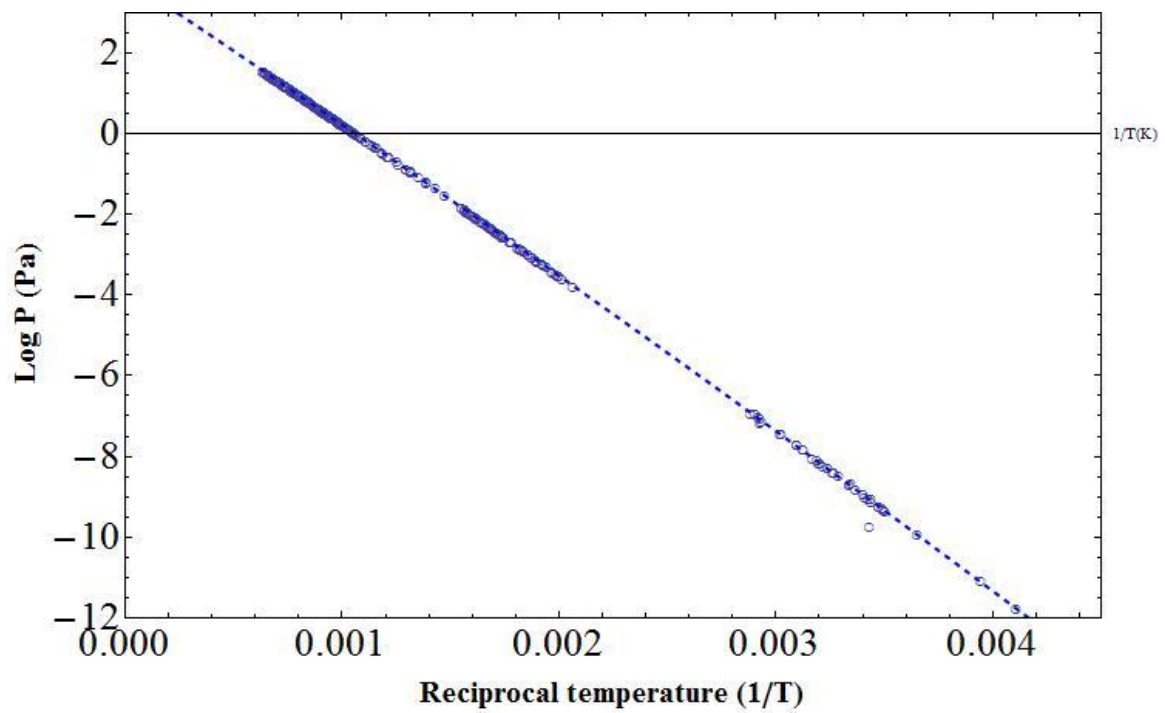


Figure 3.1.3 – Clausius-Clapeyron fit for cesium literature data

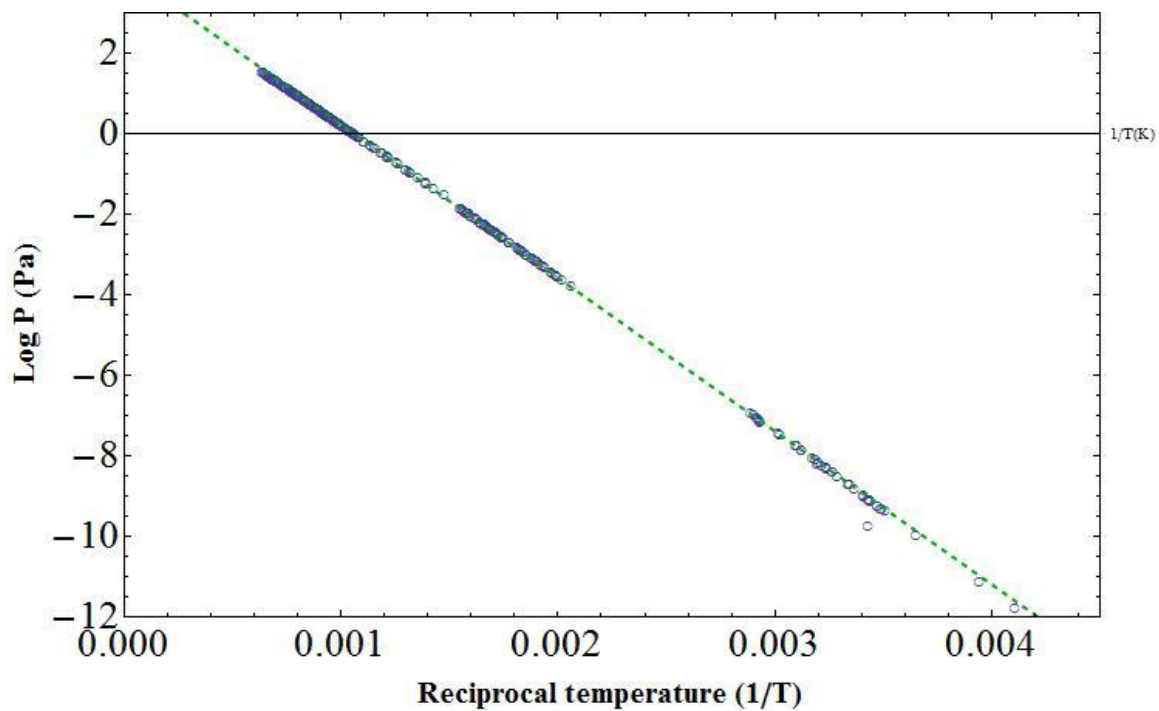


Figure 3.1.4 – Antoine fit to cesium literature data

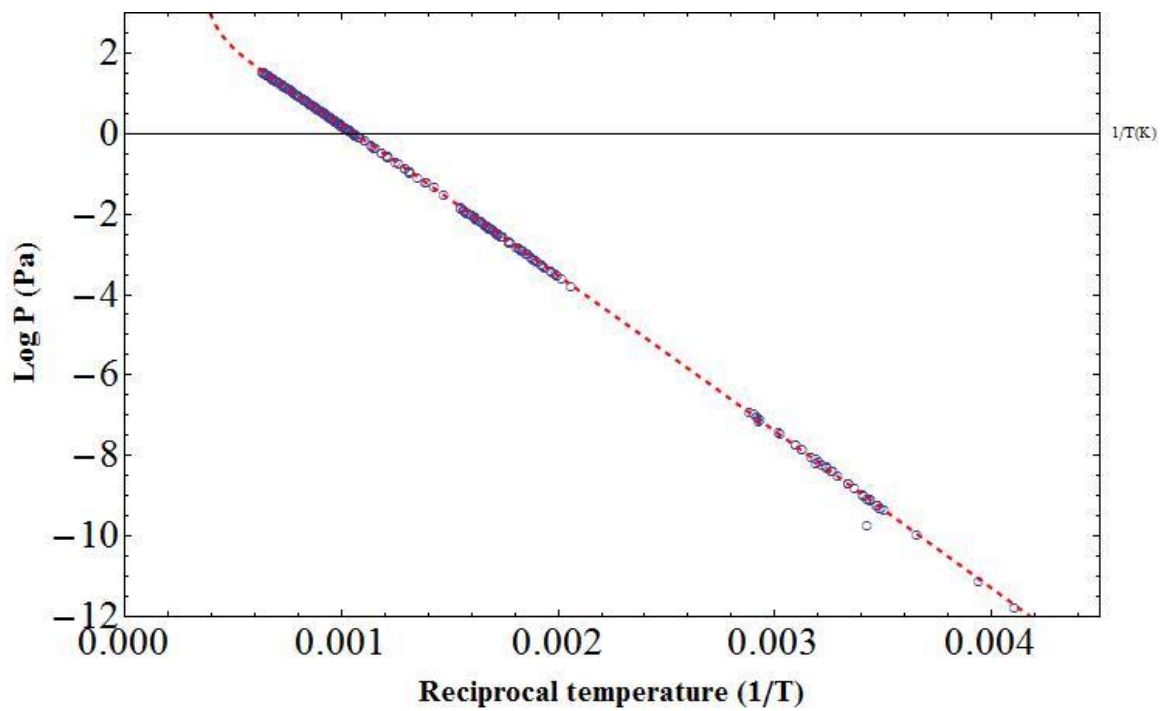


Figure 3.1.5 – Reidel fit to cesium literature data

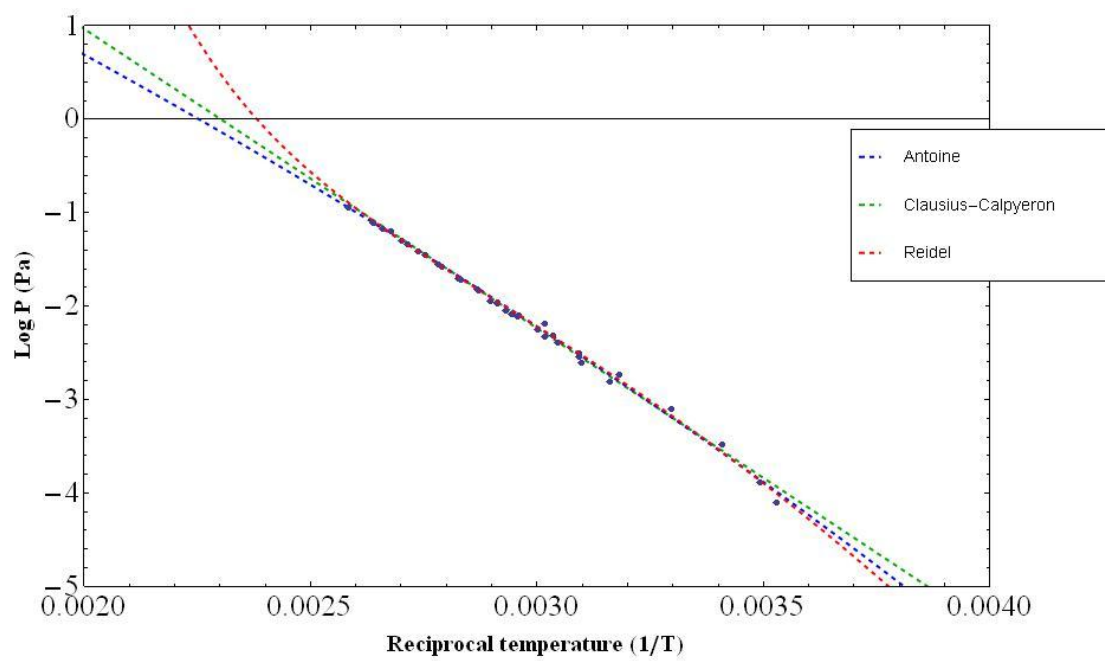


Figure 3.1.6 - Three different fits to the literature iodine vapor pressure data

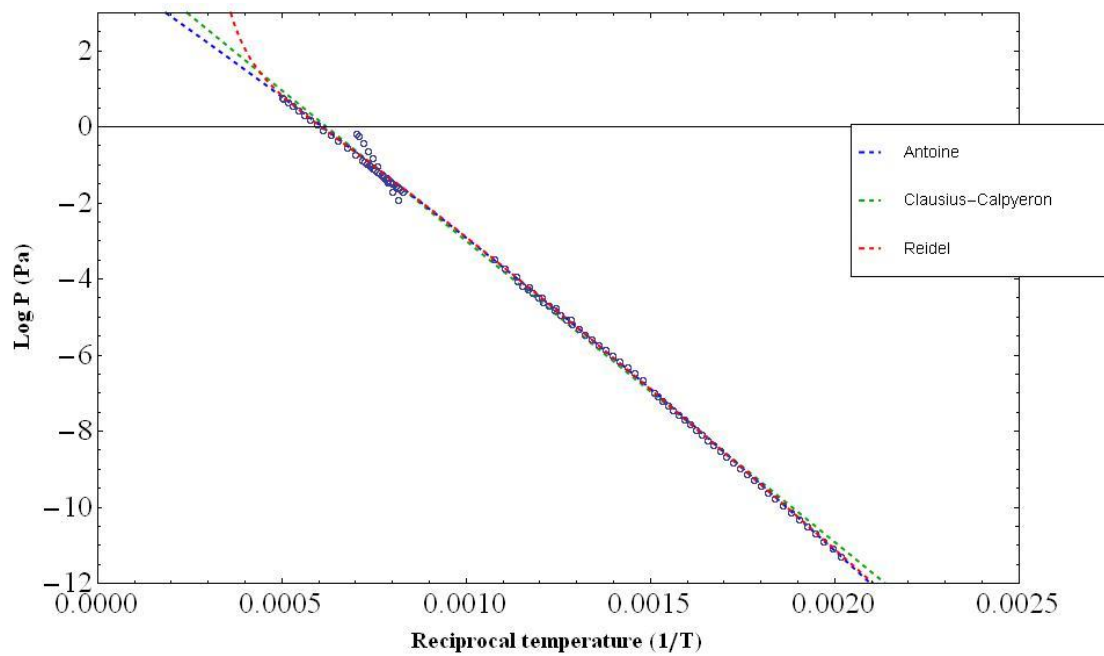


Figure 3.1.7 - Three different fits to the literature strontium vapor pressure data

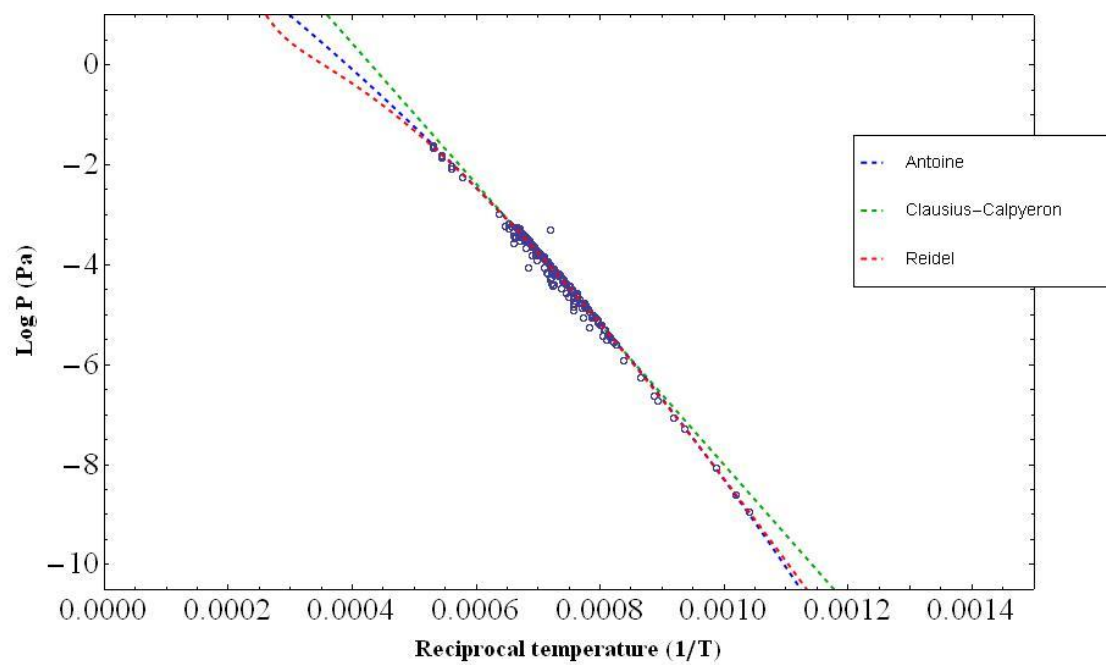


Figure 3.1.8 - Three different fits to the literature silver vapor pressure data

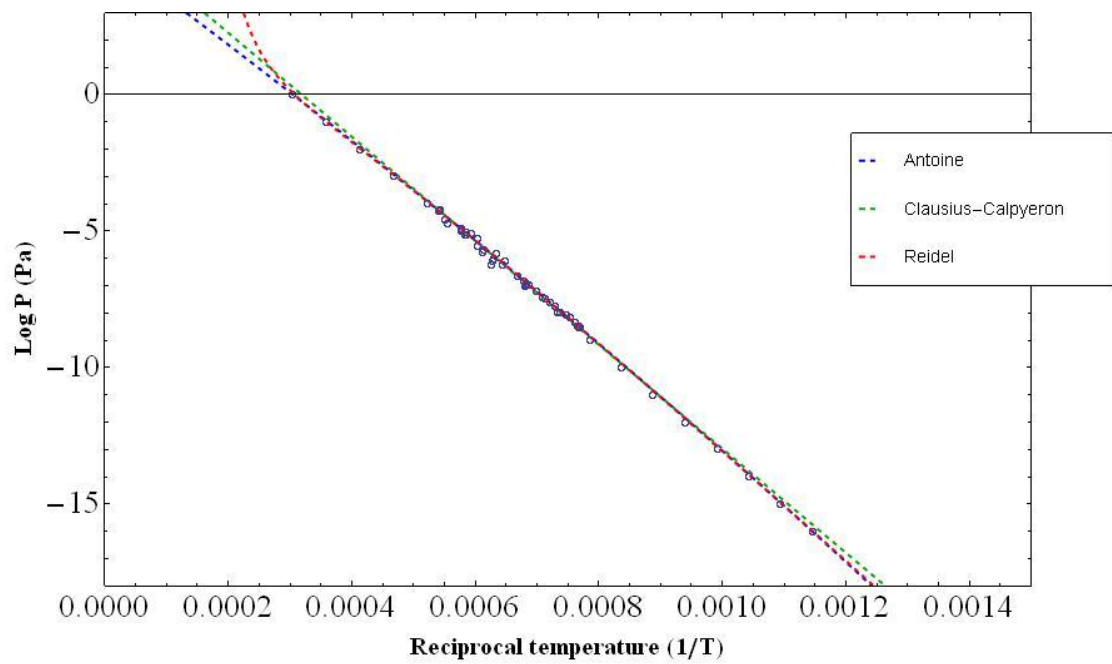


Figure 3.1.9 - Three different fits to the literature palladium vapor pressure data

Table 3.2 - Constant values and average error for literature iodine data fits

	A	B	C	D	Average error %
Clausis-Clapeyron	7.37486	3203.67	NA	NA	1.16
Antoine	5.26524	1959.3	-71.5417	NA	1.19
Reidel	5.7452	15.2772	-32.1897	140.196	1.30

Table 3.3 - Constant values and average error for literature strontium data fits

	A	B	C	D	Average error %
Clausis-Clapeyron	4.91855	7194.2	NA	NA	15.39
Antoine	4.25561	6710.39	-64.0093	NA	9.18
Reidel	18.7813	9430.3	-1.77327	3.70296×10^{-21}	1.30

Table 3.4 - Constant values and average error for literature silver data fits

	A	B	C	D	Average error %
Clausis-Clapeyron	6.04559	14049	NA	NA	2.88
Antoine	3.85448	8761.39	-279.183	NA	2.02
Reidel	54.7682	22123.7	-5.92536	2.82703×10^{-22}	1.99

Table 3.5 - Constant values and average error for literature palladium data fits

	A	B	C	D	Average error %
Clausis-Clapeyron	6.13319	19118.6	NA	NA	1.92
Antoine	5.19136	16612.6	-88.995	NA	1.15
Reidel	26.5245	22438.7	-2.48163	5.97156×10^{-22}	1.14

There are a few points worth noting from these fits. In all cases except iodine the Reidel equation gives the best fit to the available data. This is particularly true in the cases of cesium and strontium. For iodine, the Clausius-Clapeyron equation gives the best fit. This is surprising since this fit has the simplest form of all the fits used. Two possible reasons suggest themselves for this. Firstly, the data set for iodine is quite small in temperature extent. The departures from the Clausius-Clapeyron equation for the other fission products generally occur over a much wider temperature range. Secondly, it is possible that iodine more closely approximates an ideal gas than the other vapors. Since the Clausius-Clapeyron equation assumes an ideal gas, it should be sufficient to describe the vapor pressure of something that closely approximates an ideal gas.

It should also be noted that the Reidel equation typically uses the reduced temperature as a variable, rather than merely temperature. This is the temperature of the substance divided by its critical temperature. No data exists for the critical temperature of strontium, silver or palladium so this value has simply been set to one in the equation used for the fits. The relation will still hold and inserting the actual critical temperature at a later date will merely change the values of the constants.

This analysis will allow us to make the best possible determination of the vapor pressures present in our experimental system.

3.2 – Adsorption literature

The adsorption of fission products on reactor structural material is a subject of great importance for design, operation and maintenance considerations.

Although a significant body of literature exists on the subject, the majority of the literature examines the adsorption of fission products with the greatest health effects, usually for the purpose of determining how much of the fission product may be released in an accident. Most of the literature related to the adsorption of cesium is focused on graphite as the adsorbent. A similar trend can be noted for iodine. Findings from the literature are summarized in Table 1.

Table 3.6 - A summary of the literature on the adsorption of fission products on structural materials of interest in VHTRs.

Fission product	Author	Title	Year	Experimental method	Notes
Cesium	Meyers, et al ²⁸	Cesium Transport data for HTGR systems	1979	Knudsen cell mass spec and Isopiestic	Used radiotracer to determine Cs Conc's
Cesium	Holian ²⁹	The interaction between Cesium and graphite for use in the study of surface phenomena	1976	Computational study of surface effects of Cs adsorption on graphite	
Cesium	Hu ³⁰	Cesium	1986	LEED study of	Identified six

		adsorption on (0001) graphite surface		structure of Cs Adsorbed on graphite	different structural arrangements
Cesium	Phillips ³¹	Modeling of caesium deposition on CAGR reactor circuits		Radio-caesium deposition on steel	
Cesium/Iodine	Repanszki, et al ³²	Adsorption of fission products on stainless steel and zirconium	2007	EQC microbalance	
Cesium	Seyller, et al ³³	Characterization of K and Cs adsorption on Fe(110)	1999	LEED study of structure of Cs adsorbed on Fe	
Cesium	Hilpert et al ³⁴	Sorption of fission products on graphite and its influence on their release behavior in a Pebble bed HTR under accident conditions	1988	Knudsen cell mass spec and Isopiestic	Very similar to General Aomics experiments, different graphite grade
Iodine	Iwamoto ³⁵	The behavior of iodine in adsorption and desorption by graphite	1967	Radiotracer study of I adsorption on natural graphite	
Iodine	Osborne, et al ³⁶	Iodine adsorption on steel in Helium	1979	Radiotracer study of I adsorption on steel	
Strontium	Hilpert ³⁷	Sorption of strontium by graphitic materials	1985	Similar to Cesium study	
Strontium	Myers ³⁸	Strontium Transport data for HTGR systems	1974	Similar to Cesium study	

The IAEA conducted an extensive analysis of Fuel performance and Fission Product Behavior in Gas Cooled reactors (TECDOC 978). This document summarized most of the literature existing at the time on adsorption of fission products (and many other areas relating to gas cooled reactors). The majority of the work was done at General Atomics (GA) in the US by Myers and Bell, and Hilpert on German graphite.

Our conclusions from the current literature review are

- The fission product concentration level in the VHTR system is generally extremely small. As a result conventional methods of analysis are often not possible, since the lower limit of detection for conventional instruments is significantly higher than the anticipated concentration level in the VHTR. The radiotracer method was found to be the method of choice, since it can detect very low concentration levels.
- A large number of adsorption studies have used radiotracers in various ways to calculate fission product concentrations on graphite and other structural materials. While these studies are methodologically sound, the use of radiotracers introduces a potential source of error through the associated counting statistics. The concentrations of fission products in these studies are always very small, so these errors may become significant.

- Another important issue is the variability that has been observed in the adsorbed amounts of fission products (notably, cesium) on different grades of graphite. Hilpert notes that there is a difference of two orders of magnitude between the adsorbed quantities he found on German A-3 matrix graphite compared to the quantities found by Myers on US graphite grades. For this reason, it is desirable to make measurements on modern grades of reactor graphite that may be used in new VHTR's, for example, the PBMR.
- It has also been noted that there is a lack of data for multi-component adsorption. In an actual reactor core, none of these fission products exist independently of the others. It is thus very desirable to study their adsorption in combination.
- In addition to the need for more data, there is a need to attempt to model these adsorption processes more accurately. The current models used in accident simulation codes use models containing many arbitrary constants that have to be experimentally determined, and vary considerably between studies. Preliminary examination of the available data suggests it may be possible to model these processes without the need for so many arbitrary constants.

3.3 – Analysis of GA data for cesium adsorbed on graphite

The model used by Myers and Hilpert as reproduced in the IAEA TECDOC³⁹ is as follows.

$$\ln p_F = \left(A + \frac{B}{T} \right) + \left(D + \frac{E}{T} \right) \ln c_{gr} \quad (3.3.1)$$

$$\ln p_H = \left(A + \frac{B}{T} \right) + \left(D - 1 + \frac{E}{T} \right) \ln c_t + \ln c_{gr} \quad (3.3.2)$$

$$p = p_F + p_H \quad (3.3.3)$$

$$\ln c_t = d_1 - d_2 T \quad (3.3.4)$$

Where p_F is the Freundlich isotherm vapor pressure contribution of the fission product, p_H is the Henrian contribution, c_{gr} is the concentration of the fission product on, in this case, graphite, c_t is the concentration at which the adsorption transitions from Henrian to Freundlich, A, B, D, E, d_1 and d_2 are constants determined by experiment.

The adsorption data of cesium on H-451 graphite at different temperatures as reported by GA is plotted in figure 3.3.1. These data show characteristics typical of physical adsorption; the adsorption capacity decreased with the increase of temperature. If cesium is physisorbed on graphite, it may be desorbed from the graphite surface either by reducing the partial pressure of adsorbate in the gas stream, i.e., by flowing pure gas over graphite or by heating the sample to a

higher temperature. This would not be possible if cesium is chemisorbed on the surface.

The adsorption data were further examined by calculating the heat of adsorption in order to determine which process accounted for the adsorption of cesium on graphite at VHTR operating temperatures. The isotheric heats of adsorption can provide some indication of the nature of adsorption. Equation 2.3.17 is used to calculate this heat of adsorption from a plot of $\log(P)$ against $\frac{1}{T}$. Figure 3.3.2 shows the results of this analysis.

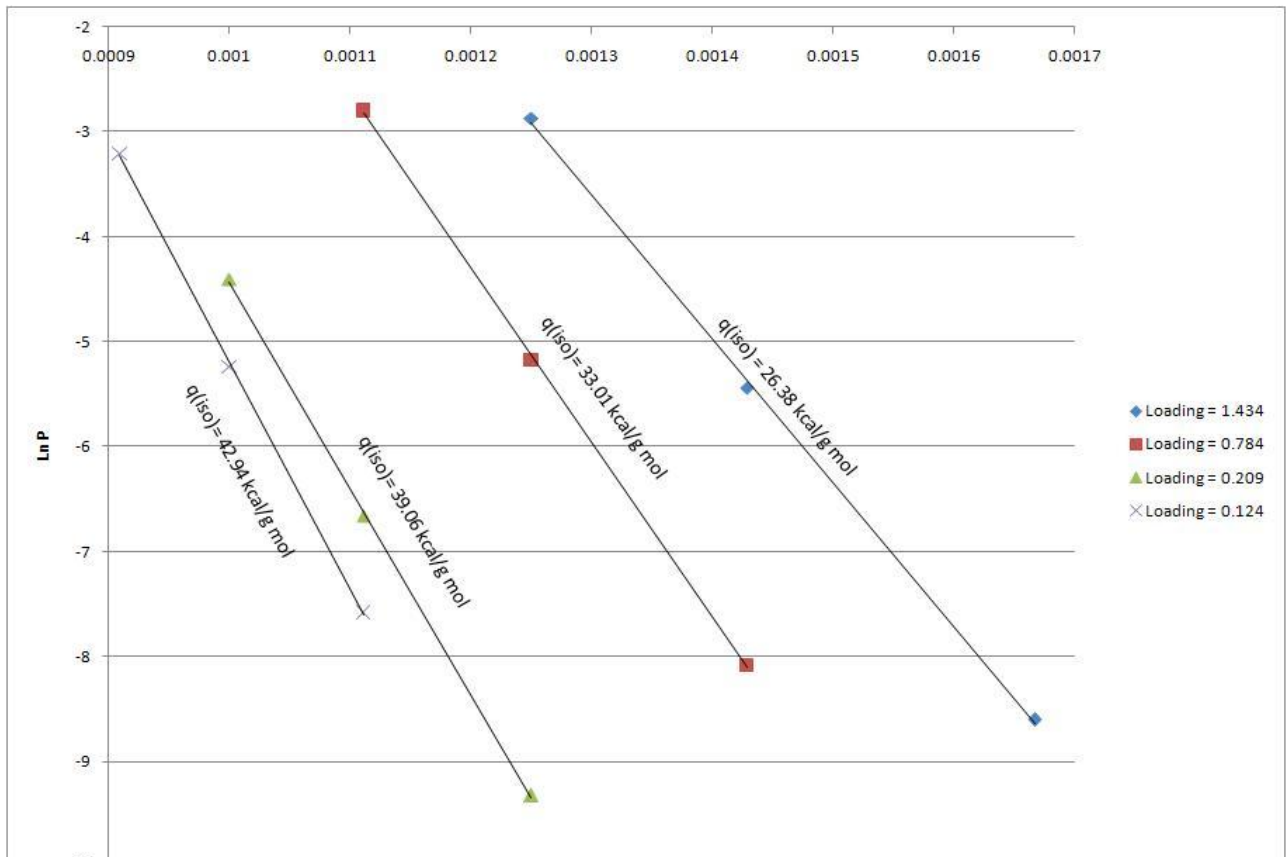


Figure 3.3.2 – Plot of isotherm calculation for different loadings of cesium on graphite from GA data

These suggest that the graphite surface was heterogeneous in nature and also the heat of adsorption increased with the decrease in loading. This is interesting since in the case of physisorption, most energetic sites will be occupied first. Therefore the heat of adsorption will be higher at lower loading, as the adsorption progresses, the heat of adsorption decreases reaching the heat of condensation. This is shown in figure 3.3.3.

In the case of physisorption, the heat of adsorption is generally in the order of 2.3-4.8 kcal/mole (10-20 kJ/mole) compared to 9.5-95 kcal/mole (40-400 kJ/mole) during chemisorptions. The magnitude of the heat of adsorption or cesium-graphite system suggests chemisorptions, while the adsorption isotherm data suggests physisorption. This reinforces the need for further experimental data as the nature of adsorption has important implications for design, maintenance and safety aspects of VHTRs.

The adsorption data were correlated according to two models; the first being the classical Langmuir equation and the second being the isotherm model suggested in the IAEA TECDOC.

The Langmuir equation was selected since the adsorption data show type I behavior. Although the heats of adsorption also suggest chemisorptions, the type I shape of the curve could be best fitted by the Langmuir equation. The experimental data and the calculated data from the Langmuir equation, along with plots of the IAEA equation (dotted blue lines) are shown in figure 3.3.4.

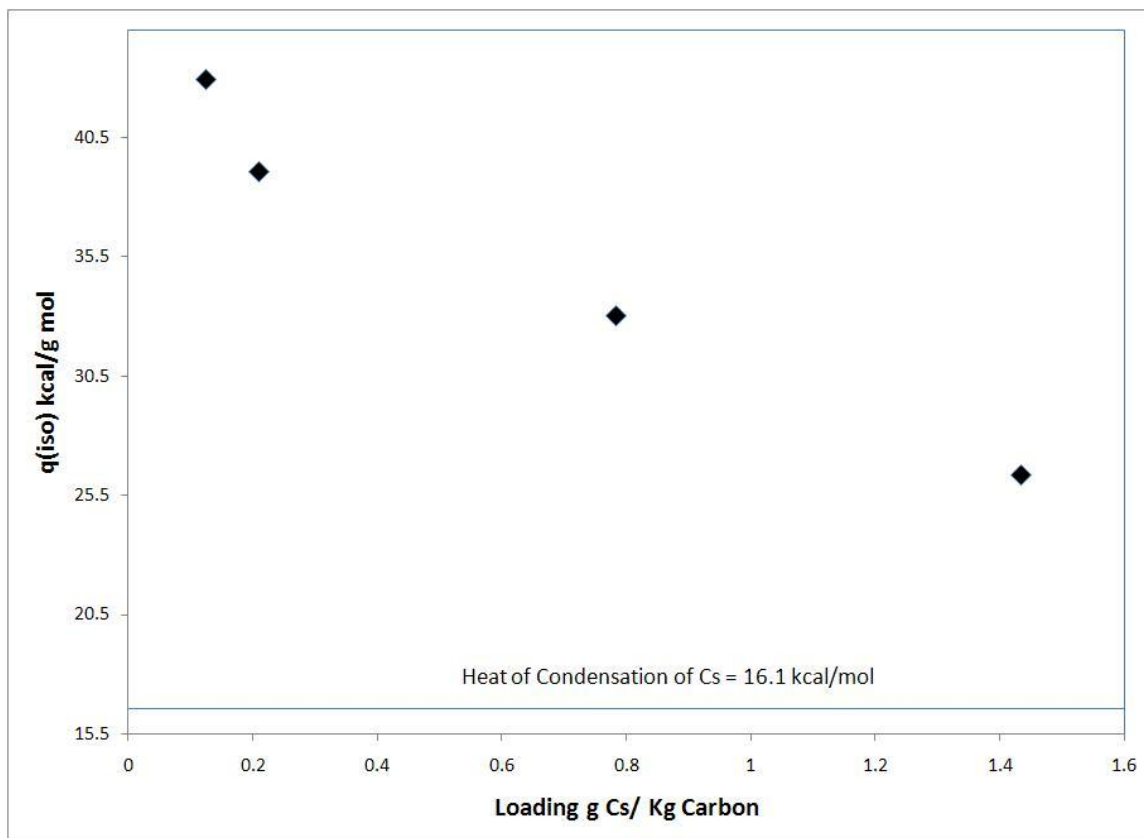


Figure 3.3.3 – Variation of heat of adsorption as loading increases. The approach to the heat of condensation is clearly discernable

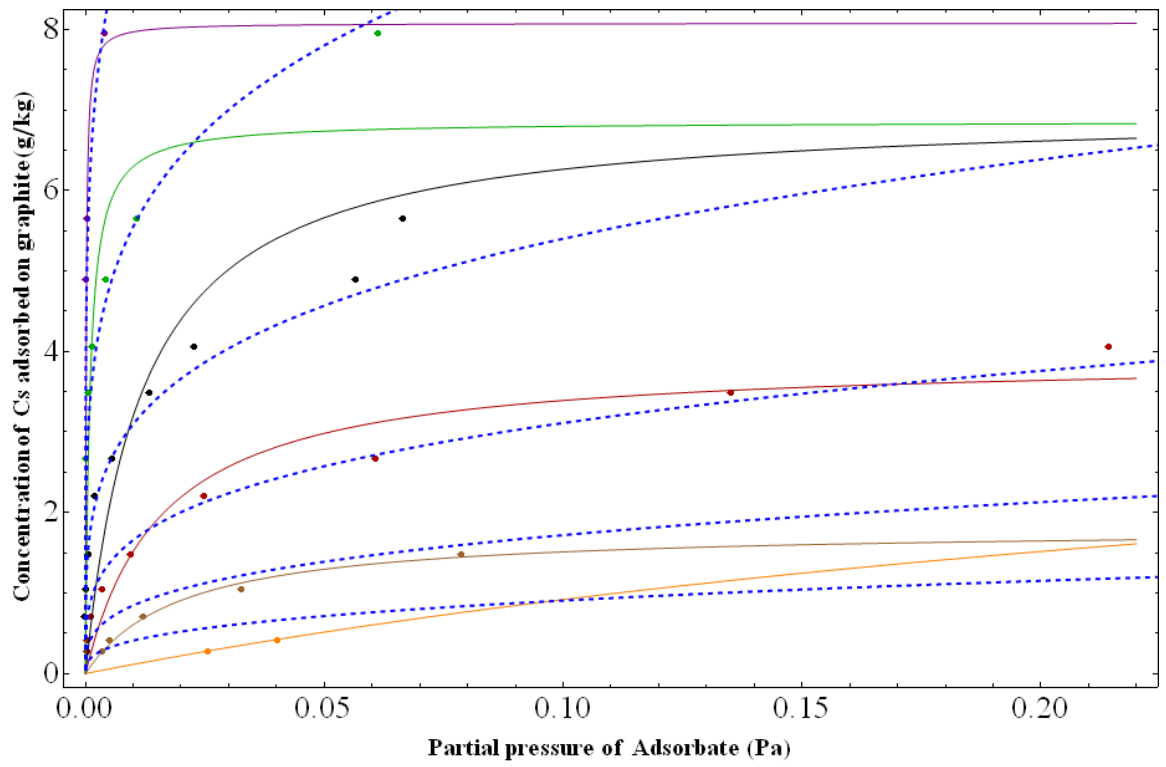


Figure 3.3.4 - GA data with Langmuir (solid colour lines) and IAEA (dashed lined) fits

These fits may be improved by disregarding some data points, but given the small number of data points available, this has not been done here. A Langmuir isotherm requires only two constants, and so may be a much better model than the existing model, containing as it does, six arbitrary constants that must be determined from experiment. It can be seen that the Langmuir fits are neither significantly better nor worse than the IAEA model in most cases. Given the extra parameters needed for the IAEA model, it may be preferable to use a Langmuir isotherm to describe this data. More data is needed in order to more fully compare these models.

Chapter 4 - Experimental Design

4.1 - Introduction

Our intention in this work is to design a system capable of measuring the adsorption of the fission products we have selected on VHTR structural materials.

The description of the experimental setup is given below. There are several sections within the experimental system that needed to be designed carefully.

The first is designing an experimental system capable of producing the extremely low concentrations of the fission products that will be present in VHTR cores. The samples of structural material should be exposed to this low concentration. There are a number of steps to be considered in achieving this experimental setup, not least of which is avoiding the plateout of these vapors on the components of the experimental setup prior to the point where the structural material being studied is exposed. Since the vapor pressure varies considerably from fission product to fission product, the heating of different parts of the experimental setup to an appropriate temperature is critical. In this work, iodine has been produced in very low concentrations, well below its saturation point at low temperatures, by the heating of permeation tubes. Cesium vapor has been produced by heating a metal sample at temperatures between 30°C and 90°C. Cesium is highly reactive

with water, and so extreme care must be taken in its use since it is flammable in air (due to moisture content) and reacts explosively with water.

All other fission products need to be heated to temperatures in the range of 500 - 2000°C to produce significant amounts of vapor. This presents difficulties in maintaining their vapor in a gas stream without plateout since an extremely high dilution factor will be needed for the vapor-gas mixture to dilute the fission product vapor to a point where it will not plate out on the tubing of the system when the tubing is heated to an achievable temperature. In theory, the entire system including the tubing could be heated to a temperature sufficient to prevent the fission product from condensing on the system prior to exposing the sample, but in practice this becomes extremely difficult with increasing temperatures.

Avoiding the plateout of these vapors prior to exposing the sample can be controlled by diluting the gas stream so that the partial pressure of the fission product vapor remains below the saturation pressure for that vapor at the temperature of the gas stream (which will be different from the temperature in the furnace where the vapor is produced). Additionally, the tubing through which the vapor laden gas will flow can also be heated so long as the required temperature is not too high. Depending on the fission product being studied, one or both of these methods are used.

4.2 – Analysis methods

The second major challenge in this work is in quantifying the amount adsorbed on the structural material samples. Several methods can be used for determining the amount of fission products adsorbed on the sample.

4.2.1 – Thermo gravimetric Analyzer

The first method of analysis involves measurement of the weight change of the sample as it is exposed to fission product vapor in a Thermo gravimetric Analyzer (TGA). The TGA is a sensitive electro-balance that suspends a sample in a hanging bucket contained within a furnace. The sample can be heated to the desired temperature, and any weight change in the sample can be detected down to microgram amounts. So long as the sample adsorbs several micrograms of fission product, the TGA is able to quantify this.

Figure 4.2 is a schematic of the balance for the TGA system. The balance is a see-saw arrangement with the sample bucket hanging from a hang-down extension wire on one side of the arrangement (the left side in the diagram) and a tare bucket hanging from the other side. The pivot point at the center is connected to a sensitive electric motor. The motor acts to cancel any torque

produced when one side of the arrangement is heavier than the other. The motor supplies a counter torque, and the arrangement returns to a neutral equilibrium.

The magnitude of the current the motor draws to make this correction is proportional to the mass difference between the two sides and so, once calibrated, the balance measures the mass change taking place within the sample bucket or tare bucket, however, there should be no mass change in the tare bucket.

The tare bucket on the right side of the balances serves to mechanically compensate for the weight of the sample bucket on the left side. Without this, the motor would constantly be applying a significant torque to cancel the weight of the sample bucket. In practice, the weight of the tare bucket and sample bucket will not be the same. So long as they are somewhat close, however, the balance is able to use most of its available power to measure mass change in the system rather than merely supporting the sample bucket.

The hang-down extension wire allows the sample bucket to be suspended some distance below the TGA, in the furnace. The balance itself is sensitive to heat and so it is desirable to reduce the temperatures it is exposed to. For this reason and as a means of keeping potentially corrosive reactants out of the balance, a purge stream of helium constantly flows into the balance and down the reaction tube to ensure little heat and no contaminants flow up the reaction tube from the sample bucket to the balance.

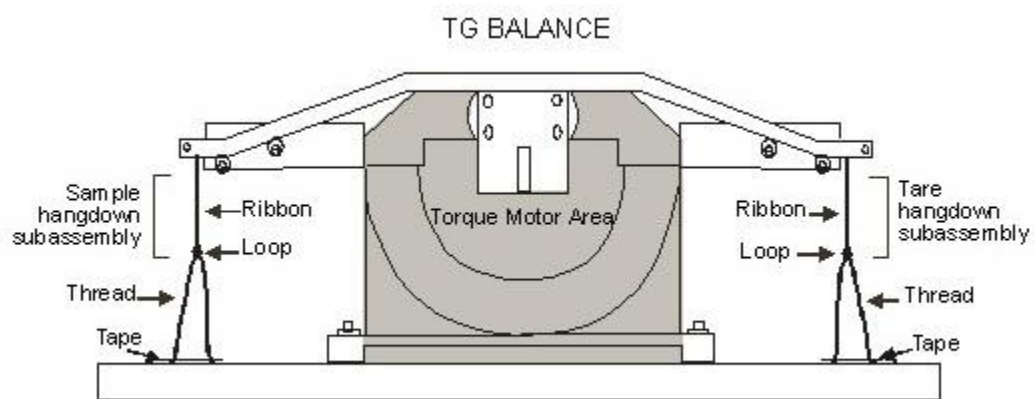


Figure 4.2.1 – Schematic diagram of the balance component for the TGA system

reproduced from Thermofisher's TGA manual

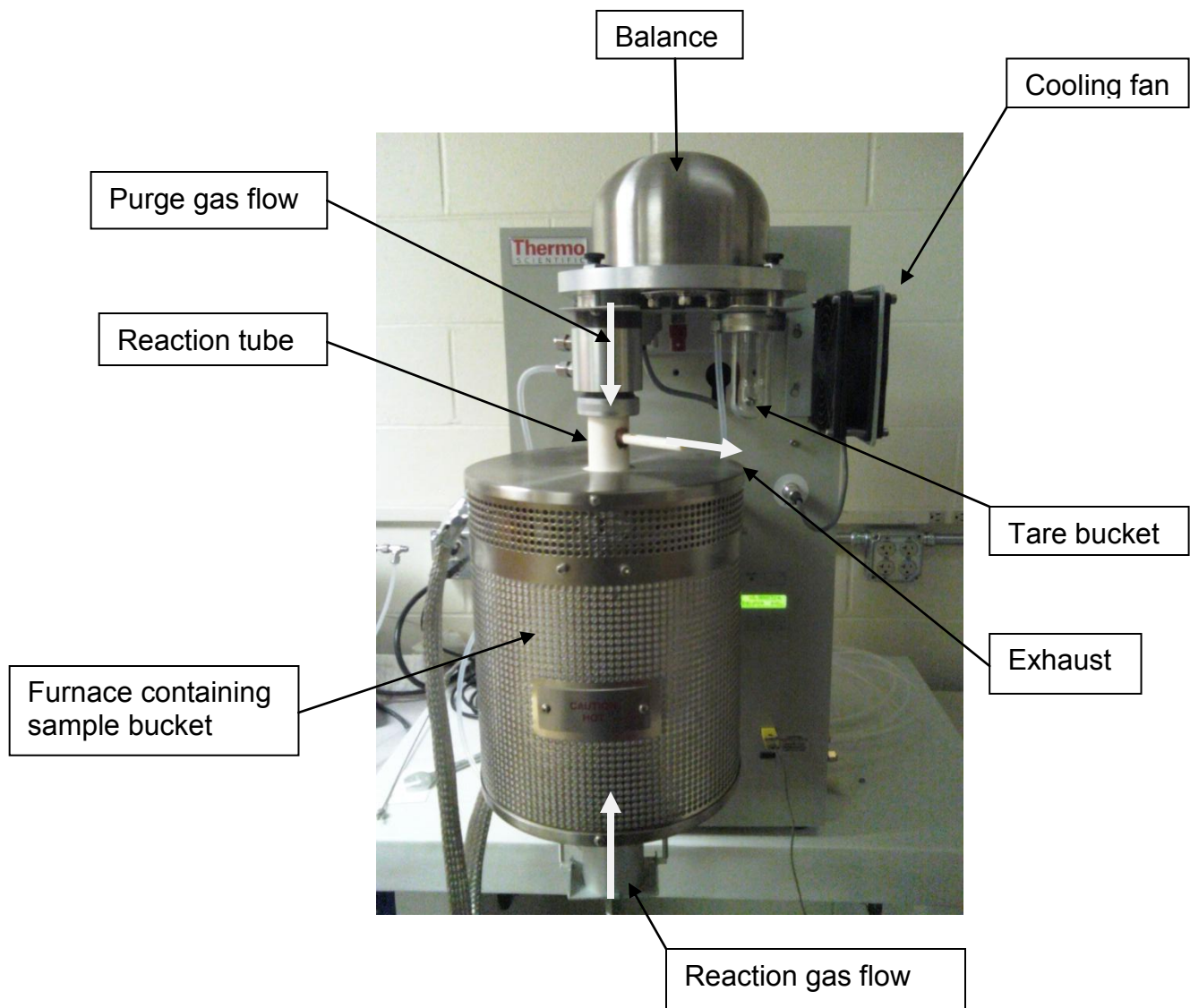


Figure 4.2.2 – Complete TGA system

The TGA system sits on a marble table weighing approximately 1000 lbs in order to isolate it from vibration. The exhaust from the reaction tube is generally vented to a series of bubblers filled with either water or nitric acid depending on what fission product is being used in the system.

It is usually necessary to make blank runs with the system before or after a sample run because as the temperature inside the furnace tube increases, the buoyancy of the gas flowing through the tube and partly supporting the sample bucket decreases. The system sees this loss of buoyancy as a weight increase of the sample. In order to compensate for this, it can often be necessary to subtract a blank run (for our purposes, blank means a run where there should be no adsorption taking place) from a sample run. This is not always necessary since it can often be the case that we wish to record mass loss once a sample reaches the desired temperature for the sample run. At this point, the buoyancy effect will have reached a constant value, and we can record any further weight change. This is often the case during oxidation sample runs where we wish to measure the oxidation rate of a sample over time.

4.2.2 – Neutron Activation Analysis

A second method of analysis is neutron activation analysis (NAA). NAA involves irradiating a sample that has been exposed to fission product vapor in the University of Missouri Research Reactor (MURR) and then performing gamma spectroscopy on the irradiated sample to quantify the amount of fission product present. This method is very sensitive; depending on the fission product, the detection limit may be on the order of nanograms. There are two main difficulties with this method. The first is that the method relies on the fission products being activated in the reactor. This happens to a greater or lesser degree between fission products, depending on their capture cross sections for thermal neutrons. Some fission products, for example, iodine, require very short irradiation times in order to be detectable (mere seconds in the case of iodine), while others can require months of irradiation to reach detectable activation levels (cesium). The second difficulty is the activation of the structural material itself during the process. This is problematic for two reasons; firstly, if the structural material is significantly activated by irradiation, it can become a radiation hazard itself. Secondly, the more activity produced in the structural material, the more difficult it will be to resolve the fission product from the background spectrum of the activated structural material. In our case, both of these difficulties are more prominent with stainless steel as a structural material than with graphite. It is

likely other metallic structural materials (such as Hastelloy X) may have similar issues to stainless steel.

4.2.3 – Inductively Coupled Plasma Mass Spectroscopy

Inductively coupled plasma mass spectroscopy is a potentially very accurate and sensitive method of analyzing samples. The system works by vaporizing a sample in argon plasma and sending this vapor to a mass-spectrometer. The argon plasma is produced by surrounding an argon tube with an induction coil the current through which oscillates at radio frequencies. A spark is generated in the argon, introducing free electrons that are then accelerated by the oscillating magnetic field produced by the induction coil. The direction of this field reverses at the frequency of the induction coil, causing the electrons to reverse direction. The oscillating electrons move through the argon gas, striking the gas atoms and causing further ionizations. The process continues until the rate of electron production in the gas matches the rate of recombination of electrons and argon ions. When this equilibrium is reached, the temperature of the argon plasma is on the order of 10,000 K.

The sample being introduced into the plasma is generally in a liquid form. The liquid is passed through a nebulizer so the droplets are easily vaporized by the plasma. The vaporized sample then flows into a mass-spectrometer, generally of

quadrupole type, where the ions are collected based on their mass to charge ratio.

Argon is chosen as the plasma for several reasons. It is the cheapest of the noble gases to produce, and its ionization potential is extremely high. It is important that the ionization potential of the plasma be as high as possible so that it is capable of fully ionizing any sample introduced into the instrument.

In the case of this work, the samples sent for ICP analysis will all be solid. Most often this will be a fission product adsorbed on a graphite or metal sample. Even with a microwave digester and boiling nitric acid, it is not possible to get the graphite samples to completely dissolve so that they can be introduced to the ICP system through a nebulizer. This turns out to not be a significant obstacle, however, since graphite is quite porous. As a result, while the graphite sample itself may not dissolve, the boiling nitric acid will dissolve everything that has adsorbed on the graphite. The adsorbent will then be nebulized and run through the ICP.

ICP is very sensitive as a result of its use of mass-spectrometry. There are certain elements the system has trouble detecting, particularly those with a mass close to that of argon or argon dimers, but for elements like cesium, the detection limits can be as low as nano-grams per gram.

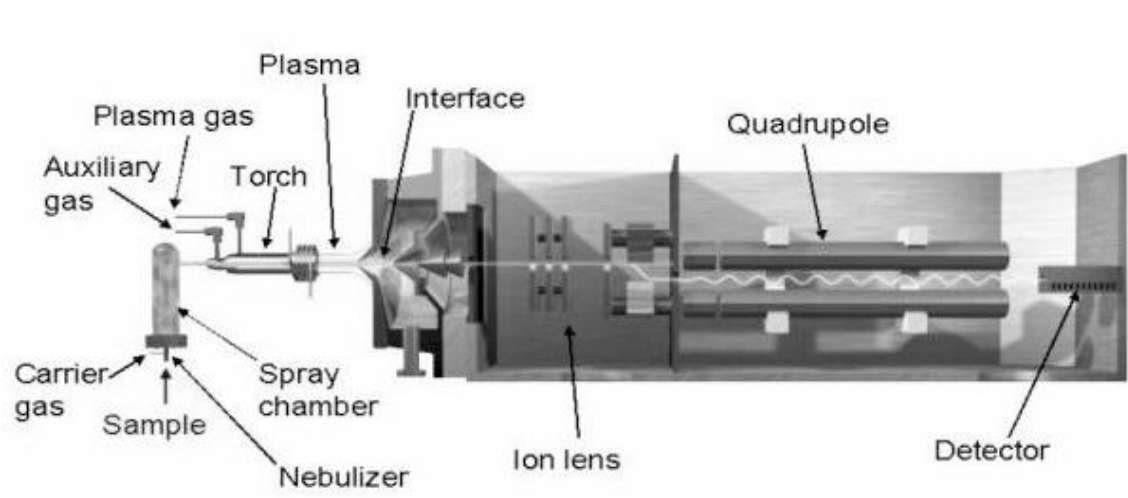


Figure 4.2.3 – Diagram of typical ICP-MS system from

<http://www2.fiu.edu/~almirall/Lecture19.pdf>

4.2.4 – Energy Dispersive Spectroscopy

Energy dispersive spectroscopy (EDS) is often a component of scanning electron microscopes (SEM). An electron beam is directed at a sample and, using the SEM, can be placed on specific sites on the sample that may be of interest or scanned across the sample in some fashion. The electrons from the beam cause electrons in the sample material to be ejected. The resulting vacancies in the electron shells are then filled by electrons from higher shells cascading down to fill the vacancy. These transitions produce X-rays that are characteristic of the element in which the transition occurs.

The emitted X-rays are then detected by the EDS equipment, usually using a solid state detector like a lithium drifted silicon detector. The detector and associated electronics characterize the incoming X-rays by energy and an energy spectrum for the sample is produced.

This form of analysis will sometimes be useful to us for certain types of sample analysis. Generally, our adsorbed amounts will be too small to see with an SEM, or detect with EDS but EDS has proved useful for identifying elements in samples that have been subjected to vapor pressures of adsorbate above saturation pressure where condensation may have occurred, as was the case in certain cesium iodide samples. It is also an very useful method of analysis for oxidation studies where we wish to analyze the surface composition of oxidized

samples. Changes in concentrations of surface species can also be studied making it possible to measure which species in an alloy may be oxidizing faster than others. With proper preparation and alignment, it can also be possible to use EDS to measure depth profiles for oxidized samples where we wish to know how thick an oxide layer may have formed.

4.3 – Experimental Setups

4.3.1 – Setup for initial testing

Initially a simplified version of our intended final setup was constructed to make some preliminary measurements. A schematic of this setup appears in figure 4.3.1.

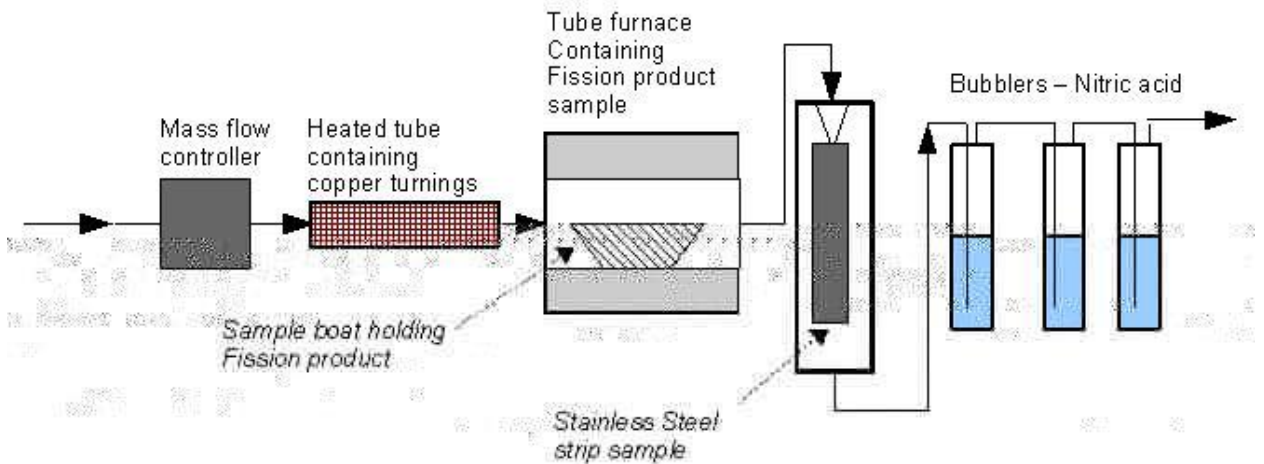


Figure 4.3.1 - Initial testing setup

The first half of the setup supplies fission product laden gas (nitrogen in this case) to the second half of the setup containing the sample of structural material. A vertical stainless steel tube was used to contain a hanging sample of stainless steel foil. Cesium iodide vapor was produced in the furnace tube and flowed into

the stainless steel tube, over the foil and exited into three of glass bubblers containing nitric acid, whose purpose was to trap the remaining fission product not adsorbed on the stainless steel strip for possible later analysis and also to prevent it from venting into the lab atmosphere. The major problem with this setup was that it was not possible to control the temperature of the stainless steel strip hanging in the tube. As a result, the strip remained at some unknown, low temperature throughout the run.

4.3.2 – TGA Setup

The preceding setup allowed us to make some simple measurements and to test that the system would work, conceptually. However, in order to quantify the amount of adsorption taking place it is necessary to know accurately the temperature of the adsorbent during the experiment particularly since we wish to produce a series of isotherms. The TGA with its furnace allows us to do this extremely accurately. Once the TGA was acquired, the previous setup was modified to incorporate it. The TGA replaces the steel tube as a sample chamber; its furnace and thermocouple allow the sample to be heated to the desired temperature while the temperature can be carefully monitored and controlled. Figure 4.3.2 shows a schematic of the TGA setup and figure 4.3.3 shows the actual setup.

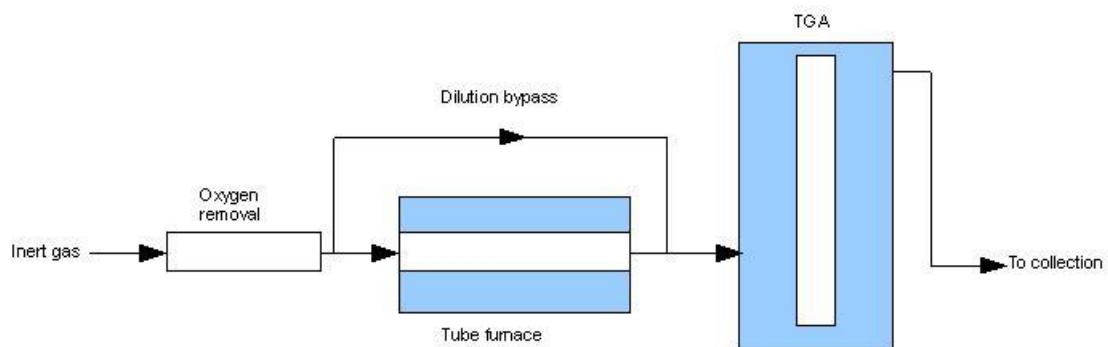


Figure 4.3.2 – TGA system setup schematic

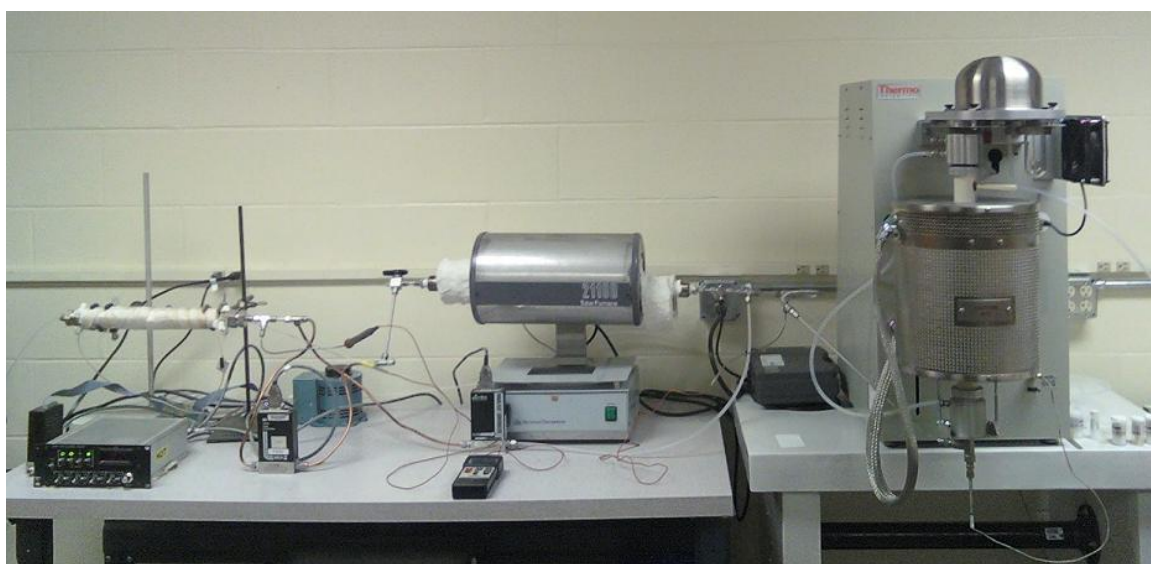


Figure 4.3.3 – TGA system

This system was used in this form to adsorb cesium onto graphite samples. Cesium is the easiest of the fission products we studied to use once it is inside the tube furnace. A reasonable quantity of cesium vapor for adsorption can be produced with furnace temperatures as low as 30°C. Once this has been diluted slightly the tubing leading from the furnace tube to the TGA does not have to be heated very much to avoid plateout, if at all. This would not be the case for other fission products, with the exception of iodine.

There are simpler ways of producing iodine than using the tube furnace arrangement that is used for cesium. Iodine can be purchased in permeation tubes. These have a number of advantages over the tube furnace arrangement but the major factor in this design that suggested their use was the fact that they can produce very low vapor pressures of iodine at reasonably attainable temperatures. The permeation tube, in fact, makes it possible to produce vapor pressures significantly lower than that which would be produced if crystalline iodine had been heated in the furnace tube.

The permeation rate of permeation tubes is very sensitive to temperature changes, so a slightly different system was constructed to keep the tube at a constant temperature. Each tube is certified by the company as having a given permeation rate at 100°C and its variation with temperature is also given. A temperature bath was built to house the tube consisting of a water bath with a stirrer. The water bath contained a glass 'U' tube filled on the downstream side

with small glass spheres and containing the iodine permeation tube on the upstream side. The stirrer ensured the water bath was thoroughly mixed and therefore assisted in maintaining a constant temperature.

Gas flowed through the same oxygen removal setup as before, then into the glass 'U' tube and on to the TGA. The temperature of the bath was measured by a thermocouple, and the glass beads through which the gas had to flow before reaching the permeation tube ensured that the gas temperature was the same as the bath temperature.

One issue with using water as the bath fluid was that at the temperatures needed to produce the vapor pressure of iodine we wanted (around 80°C depending on the run), a large amount of evaporation took place over the course of a sixteen hour run. The amount of evaporation was not sufficient to affect the temperature in the bath significantly, however, but the necessary refilling between runs increased the time it would take to heat the bath to temperature between runs. We experimented with Dowtherm oil instead of water as the bath fluid, but with the system setup as it was, the oil fumed quite badly and it was difficult to adequately ventilate the area at the time. The setup was later moved to a different lab with a fume hood so these experiments could be continued but the TGA was no longer used for analysis in that setup (since the TGA is quite immobile).

4.3.3 – Cesium cell and column setup

Loading cesium into the tube furnace proved to be extremely hazardous with the system set up as it was. The issue was, as mentioned before, cesium is flammable in air and explosive in water. The humidity in the air is the cause of its flammability. If it were possible to isolate the cesium from the lab air while loading the tube this hazard could be avoided. In practice, this was achieved by breaking a cesium ampoule contained in a ceramic boat at the downstream end of the furnace tube while inert gas (nitrogen) was flowed down the tube at a fairly high flow rate. While the sample was still exposed to air, the flow of inert gas over it prevented it from igniting in most cases.

However, it was somewhat difficult to break the ampoules in that position partly due to the geometry of the experimental setup and also because the ampoule only protruded above the ceramic boat by about a third of its diameter, the ampoule laying horizontally in the ceramic boat, making it difficult to shatter without also shattering the ceramic boat. Normally glass ampoules like these are scored then the top snapped off. Because of the need to move the ampoule into the ceramic boat and inside the furnace tube as quickly as possible it was not possible to break the ampoule in this fashion.

There are several ways the ampoule could have been broken and placed into the furnace tube in an inert atmosphere. The use of a glove box filled with inert gas is

one method that may have been possible. However, doing the sample loading this way would have been time consuming and cumbersome and somewhat more critically, would leave no way of inspecting the cesium inside the tube to determine if it had been used up during sample runs.

In order to allow for the safe and efficient loading and inspection of cesium for vapor production, a cell was designed and constructed specifically for this purpose. Figure 4.3.4 is a schematic diagram of the cell design.

The cell is a stainless steel cylinder with a hollow core on a heavy circular steel base to provide additional stability. A steel plunger assembly forms the top of the cell. The plunger assembly is sealed against air ingress with two sets of rubber gaskets. The hollow core of the cylinder is penetrated radially near the top of the cylinder to create a gas inlet port and a gas outlet port. Near the base of the hollow portion of the cylinder is another radial port where a thermocouple is inserted into the base of the cell allowing for measurement of the temperature of the cesium metal in the bottom of the cylinder.

In operation, the plunger assembly is removed from the top of the cylinder and a cesium ampoule inserted. The plunger assembly is then replaced and securely bolted to the top of the cylinder. The plunger is pushed down until it contacts the top of the cesium ampoule inside the cell. The seals cause the plunger to move with some resistance so it is designed to be struck with a hammer or hand at that point to break the ampoule. Once the ampoule has been crushed, the plunger is

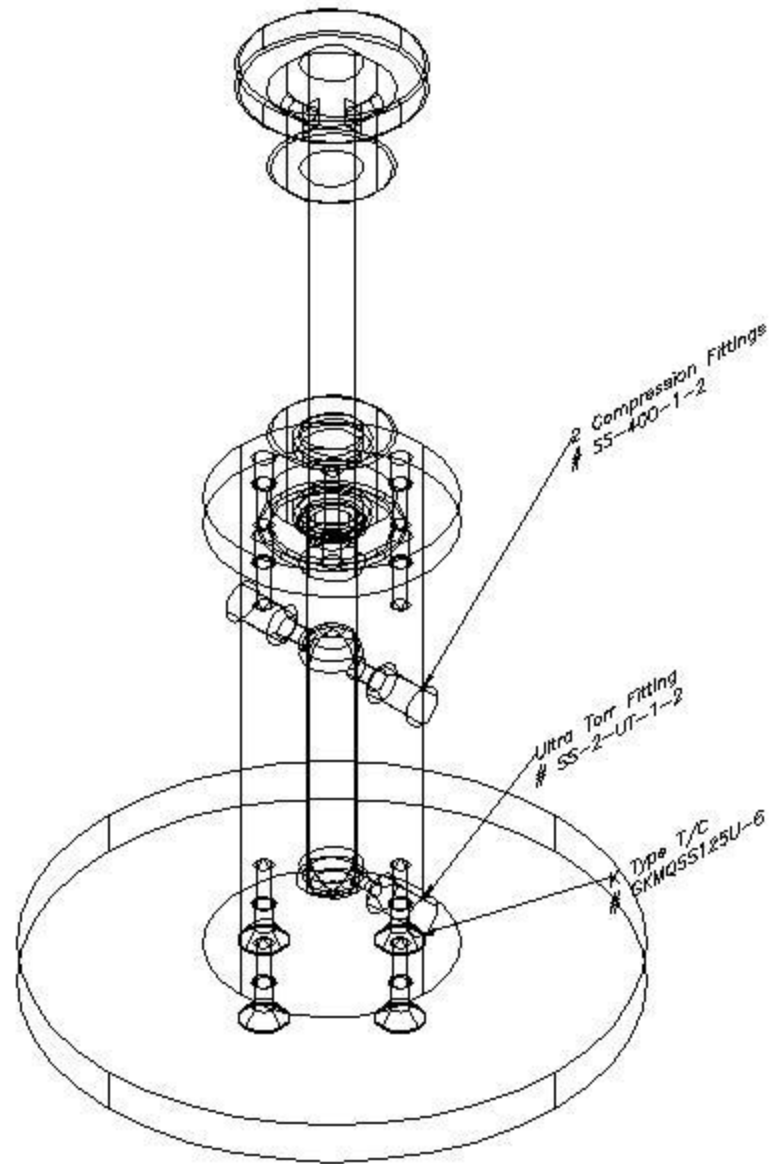


Figure 4.3.4 – Cesium vapor production cell used in this study

withdrawn to the top of the cylinder to allow the unobstructed flow of gas through the inlet and outlet ports. The cylinder is wrapped in heat tape, allowing the interior temperature to be controlled to produce the desired vapor pressure. The thermocouple in the base of the cylinder provides accurate temperature information so that the vapor pressure can be accurately determined. The flow rate of gas through the cylinder is typically very low, on the order of ten to twenty cubic centimeters per minute. The low flow rate allows the vapor inside the cell sufficient time to reach its equilibrium vapor pressure. At this flow rate, the equivalent volume of the interior space of the cylinder is flowing through the cell in approximately one to two minutes, depending on the flow rate.

By the time this system was being used, previous data had shown that the amounts of cesium being adsorbed by graphite samples inside the TGA were typically below the detection limit of the TGA. This being the case, initial tests of ICP as an analysis method suggested that we might use this as a primary means of determining the adsorbed amounts on our samples. The collection portion of the setup was redesigned in light of this to allow for a higher throughput of samples.

The TGA was replaced in this setup by three vertically mounted Inconel tubes that could be packed with graphite powder. The tubes were wrapped with heating tape and heavily insulated allowing for a maximum internal sample temperature of around 700°C as measured by thermocouples inserted from the tops of each

tube and reaching to the middle of the sample holding portion of each tube. The tubes each contained a short length of stainless steel tubing topped with a small plug of silicon insulation in the lower section of the tube. The tube and plug were placed inside the tubes in order to contain the sample in the middle of the tube where we could be most sure the samples temperature would be constant throughout its length. The vapor laden gas flowed into the bottom of the vertically mounted tubes and exited through the top where all the tubes were connected and vented to the same bubbler arrangement as before.

Since the furnace tube was no longer being used to produce vapor at this stage, and since the three Inconel tubes were capable of a maximum sample temperature of 700°C, the furnace tube was used to provide a fourth sample per run.

A simple four branch manifold was constructed to allow the gas from the cell to be split into four different sample tubes. The manifold was a simple hollow steel cylinder with an inlet port in one circular face and four equally spaced outlet ports in the opposite circular face.

Similar to all previous designs, a dilution stream joined the vapor laden gas stream immediately on its exit from the vapor producing cell. This, combined with heating the entire system with heat tape allowed us to ensure the vapor did not plateout or condense on the system prior to encountering the graphite samples.

In operation, the cell was heated to a particular temperature to produce a vapor pressure of cesium which was subsequently diluted by the dilution stream to a desired concentration. The diluted vapor then flowed through the manifold into the three Inconel tubes and the furnace tube which were heated to 500°C, 600°C, 700°C and 800°C respectively allowing for the collection of a data point at each of the four temperatures for the same concentration of cesium. Subsequent runs would then use a combination of changing the temperature of the cell and the dilution flow rate to expose four more samples to a different concentration of cesium. This allowed for the rapid acquisition of isotherm data. Figure 4.3.5 shows the setup diagram for this arrangement.

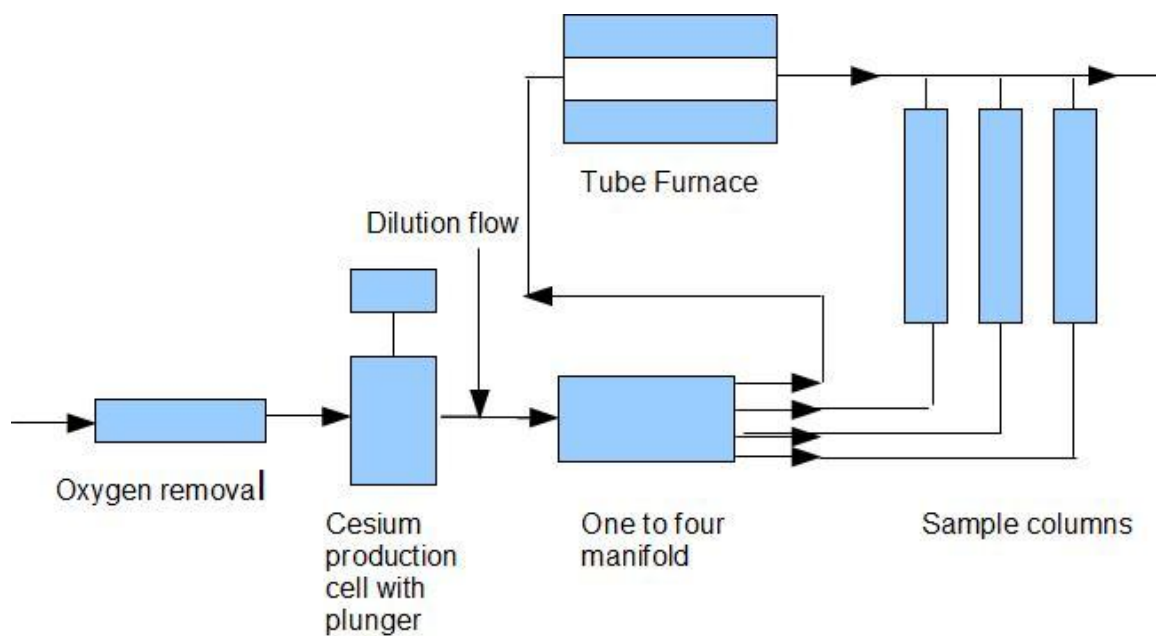


Figure 4.3.5 – Experimental setup including cesium cell, splitting manifold and sample columns

Chapter 5 - Results and Discussion

5.1 - Initial scoping experiment with cesium iodide

The setup shown in figure 4.3.1 was used to flow cesium iodide vapor over a stainless steel strip hanging in the steel sample holder tube. A ceramic boat containing several grams of cesium iodide (a crystalline solid) was inserted into the furnace tube and heated to a temperature of 650°C. This temperature was sufficient to produce a vapor pressure of cesium iodide of approximately 10 Pa. 10 Pa is an extremely high vapor pressure for experiments such as these, but this high concentration was initially used merely to allow us to get some idea of the experimental parameters. This setup did not dilute the flow of gas, nor did it heat the tubing from the furnace tube to the sample tube. As a result, significant plateout would have occurred in the tubing, reducing the concentration at the sample but the concentration would still have been very high. This run vaporized all of the cesium iodide in the tube furnace in less than an hour.

The sample strip was then analyzed with EDS. Figures 5.1.1 and 5.1.2 show the surface of the stainless steel sample as imaged by EDS.

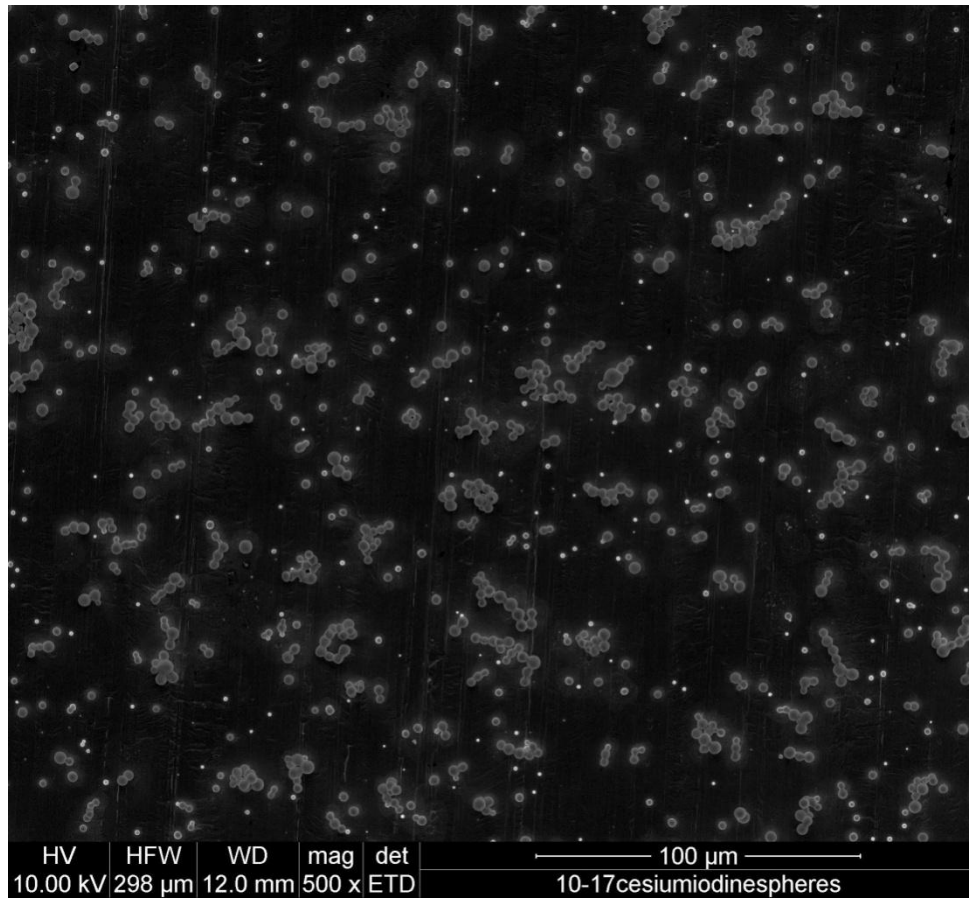


Figure 5.1.1 – EDS image of stainless steel strip exposed to cesium iodide vapor. The spheres coating the surface were analysed and found to be composed entirely of cesium iodide

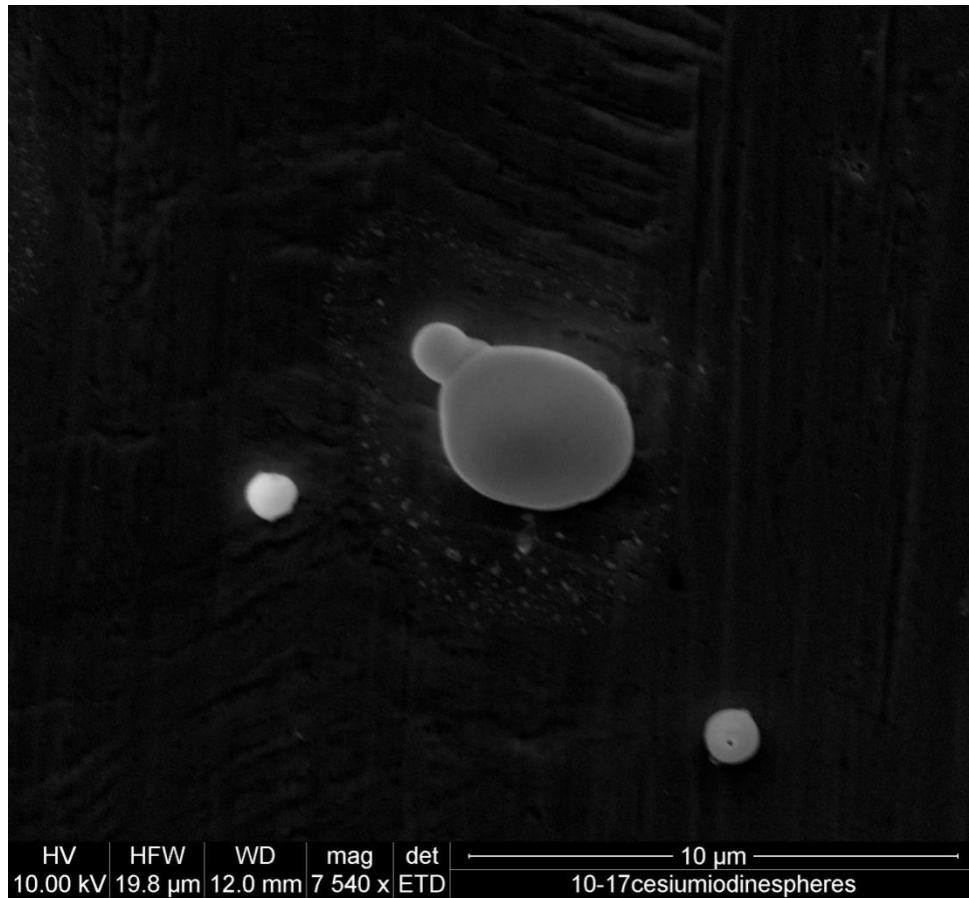


Figure 5.1.2 – A close up image of one of some of the spheres from the previous figure.

A small hole is evident in the sphere in the lower right. This was the result of the electron beam being used to analyze its composition

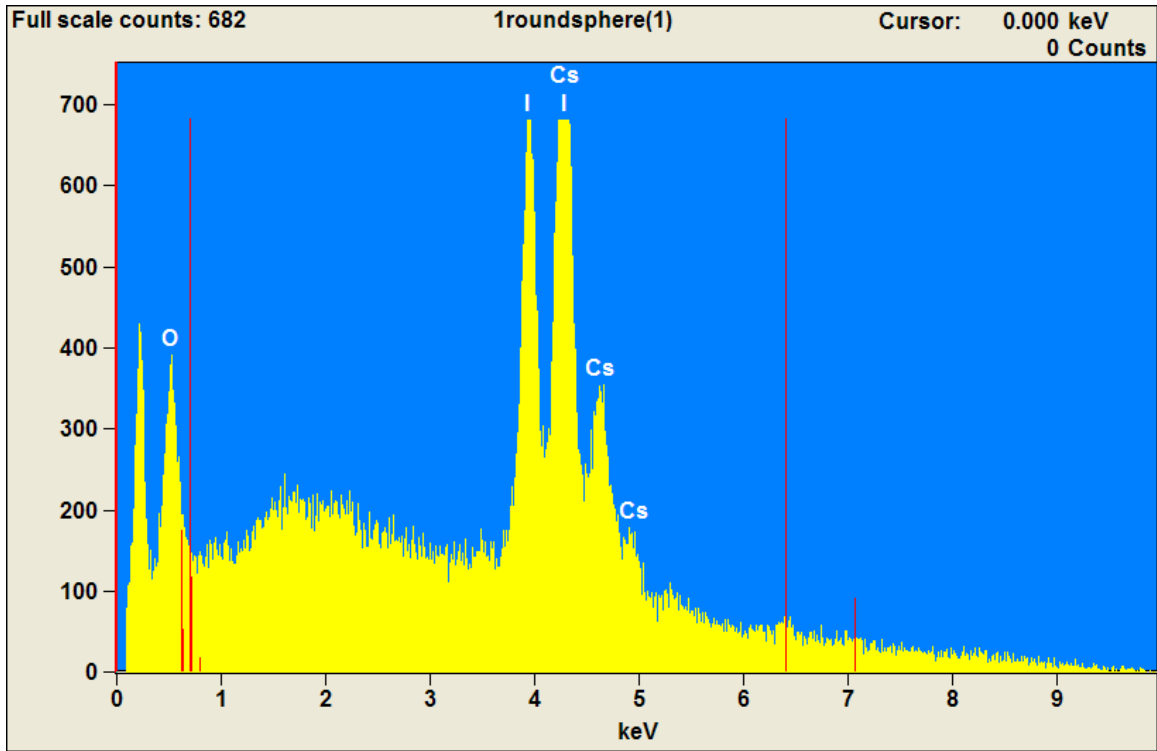


Figure 5.1.3 – EDS spectrum of the sphere from the previous figure. Elemental analysis shows the sphere is composed almost entirely of cesium and iodine

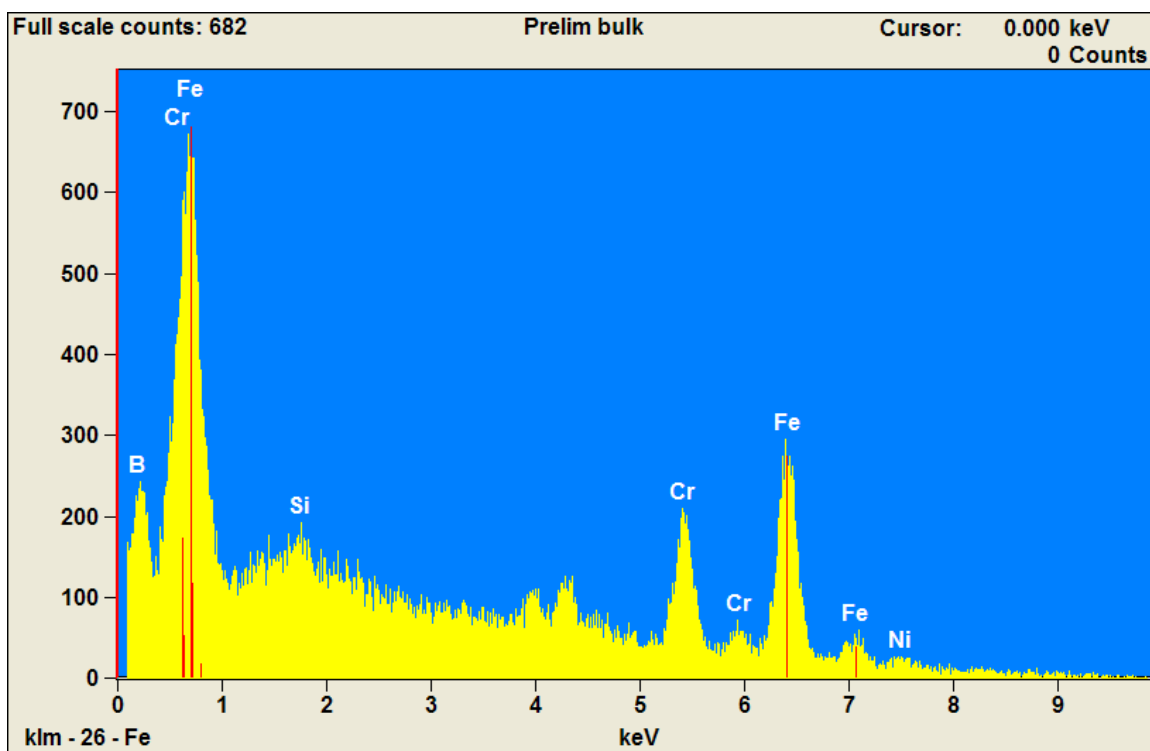


Figure 5.1.4 – EDS spectrm of the bulk material surrounding the spheres in figure 5.1.2.

The spectrum shows no cesium or iodine present indicating that the cesium and iodine detected in the spheres were, as expected, not part of the bulk material

The EDS analysis showed the metal surface was coated fairly evenly with a large number of spherical objects. Analysis of these objects showed that they were composed almost entirely of cesium and iodine. Spectra from the surrounding bulk material showed no cesium or iodine. The low temperature of the strip during this sample run, the extremely high vapor pressure of cesium iodide and the extremely localized form of the cesium iodide detected on the strip all suggest that what was observed in this experiment was not adsorption, but merely condensation.

It is possible that the bulk material did, also, contain some cesium iodide but the detection limit for EDS is on the order of hundreds to thousands of parts per million so the lack of detection of cesium iodide in the bulk material does not necessarily mean there was none, or that no adsorption whatsoever occurred.

5.2 - Iodine experiments

The setup for iodine production using permeation tubes described in section 4.3.2 was used to make some sample runs. Initially we wished to determine how long a graphite sample contained in the TGA would need to be exposed to iodine vapor in order to reach adsorption equilibrium. To this end, a number of runs were made with an iodine concentration of approximately 3×10^{-5} Pa for four, eight and twelve hours in order to establish whether there was a difference in the final

amount of adsorbed iodine detected for the different lengths of runs. No mass change was detected in the TGA, so the samples were sent for NAA. The NAA quickly revealed why the TGA has not seen a mass change.

Iodine is an ideal candidate fission product for NAA since it activates rapidly and is easily handled. The amounts of iodine detected by NAA are shown in table 5.1.

Table 5.1 – Results of NAA for iodine adsorbed on graphite for varying lengths of time

Sample ID	Sample Weight (mg)	Mass of I in Sample (nanograms)	Concentration (ppb)	Exposure time (h)
1	643.80	74.3	115.4	12
2	706.36	89.2	126.3	8
3	516.52	81.7	158.3	4
Blank	588.42	< 27.5	< 46.8	0

The TGA did not detect a mass change because the amounts adsorbed were significantly below the detection limit for the instrument. This study showed that four hours was a sufficient length of time to reach adsorption equilibrium. A gamma spectrum for one of the samples analyzed using NAA is shown in figure 5.2.1.

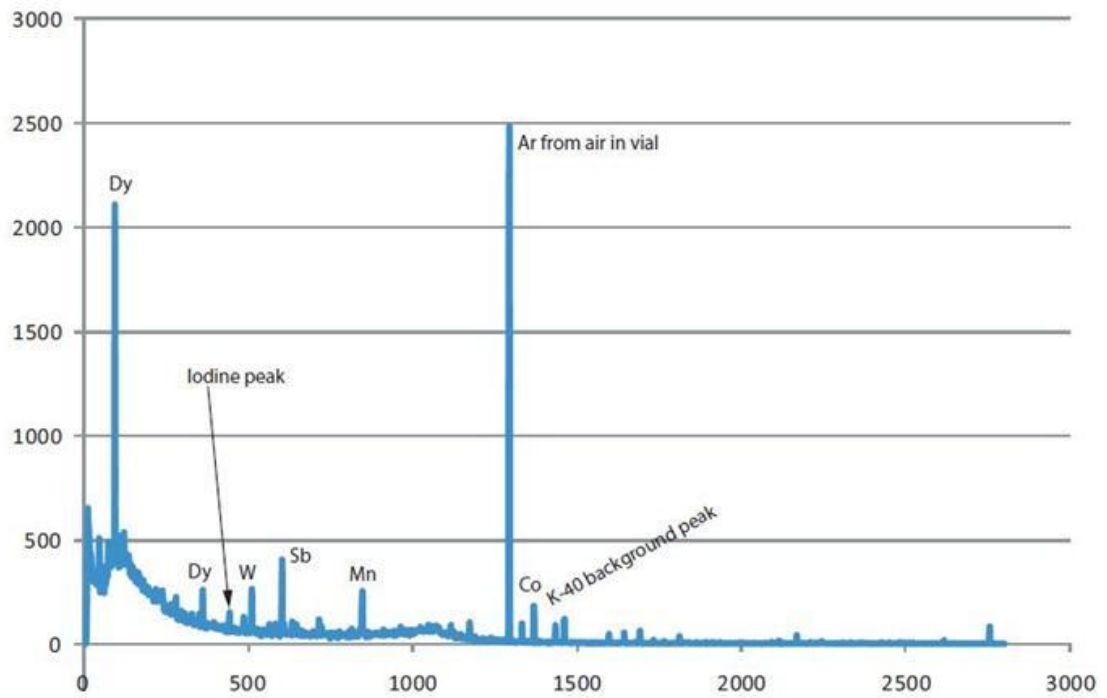


Figure 5.2.1 – Gamma spectrum from NAA on graphite samples with adsorbed iodine

5.3 – ICP analysis of cesium adsorbed on graphite in TGA

Several runs were made using the furnace tube to produce cesium and cesium iodide vapor. The TGA was used to contain the graphite samples exposed to this vapor. No consistent weight change data was produced by these runs, so it was decided to analyze the samples using ICP to see if any adsorption had taken place. This analysis was attempted at a commercial ICP lab but it was found that their equipment was not sensitive enough to detect the amounts of cesium adsorbed. They referred us to the ICP facility at the University of Missouri Research Reactor who were able to perform the analysis. The results for the three sample runs with cesium vapor are shown in figure 5.3.1. Only three samples were run since this was still a proof of concept phase but the data they produced was broadly consistent with the work of Myer at GA. The lower temperature samples adsorbed more cesium and appear to tend towards an equilibrium saturation amount adsorbed although it is not possible to conclude this definitively from the limited data. These data suggest once again that the isotherm form for this process is type 1, as observed in the GA experiments.

The samples exposed to cesium iodide were also analyzed and found to contain cesium in the hundreds of nanograms per gram of graphite range. Iodine was also detected but limitations of the instrumentation did not allow its quantification.

The TGA was unable to detect the amounts of cesium adsorbed in either case since they were in the hundred of nanogram range, an order of magnitude below its detection limit of a microgram.

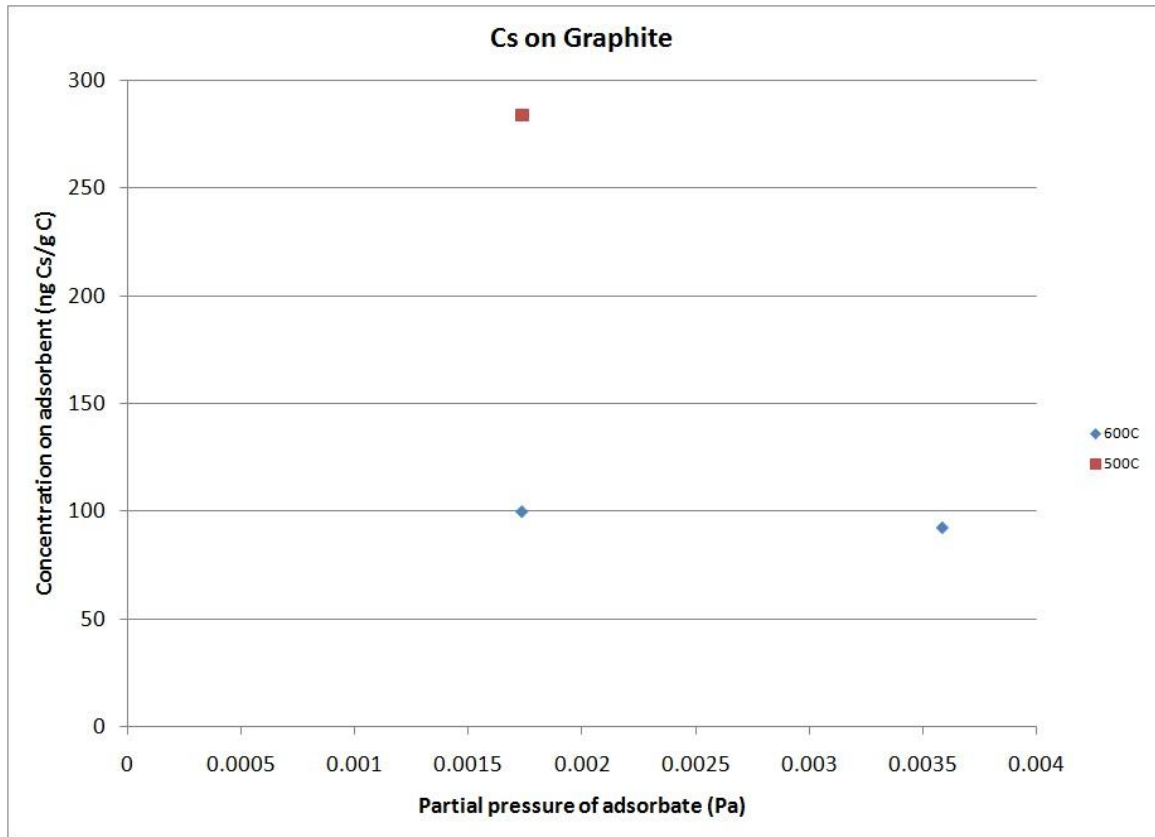


Figure 5.3.1 – Results of ICP analysis of graphite samples with adsorbed cesium

5.4 – ICP analysis of cesium adsorbed on graphite using cesium cell and inconel columns

Given the success of the ICP analysis of previous samples, the system shown in figure 4.3.5 was designed and built to allow more rapid production of samples for ICP analysis. Four samples were run at the same time, three in the inconel columns and one in the tube furnace, with the same cesium concentration. The temperatures of the samples for all runs were 500°C, 600°C, and 700°C for the three inconel columns and 800°C for the tube furnace. Each run lasted approximately sixteen hours and the cesium partial pressures ranged from 0.00013 Pa to 0.0364 Pa.

The data produced from these runs was of quite low quality. The samples contained in the tube furnace proved to be heavily contaminated and so must be dismissed out of hand. The data from the samples contained in the columns varies quite widely and several points deviate very significantly from the expected form of the data. Table 5.2 summarizes the data from the three columns.

Table 5.2 – Adsorbed amounts of cesium on graphite samples from ICP analysis

Vapor Pressure of Cesium (Pa)	Cesium adsorbed at 500°C (ppb)	Cesium adsorbed at 600°C (ppb)	Cesium adsorbed at 700°C (ppb)
0.0001365	136	89	164
0.0002241	609	61	85
0.0003802	432	214	168
0.0016679	312	575	402
0.0037781	109	184	139
0.0364732	793	838	9283

This data is inconsistent and is almost certainly the result of some systematic flaws in the experimental method. It is shown in figure 5.4.1 and 5.4.2.

The cesium vapor flowing to the samples passes through a one to four manifold before reaching the samples. The manifold is symmetric in design so differences in the flow rates through the exit branches should be minimal due to the geometry of the manifold but small differences may result. However, the packing of the inconel columns may be a problematic in this setup. While the concentration of cesium vapor will not differ among the columns, depending on the packing density of the graphite the flow rates through the columns may be significantly different. This was not thought to be a major problem since it was

expected the adsorption process should proceed quite rapidly and so variations in flow rate should not matter over the duration of a sixteen hour experiment. The data suggests this assumption is inaccurate. In loading the graphite into the columns, the graphite was simply introduced to the columns through a plastic funnel placed into the top of the tube, and the graphite was allowed to settle naturally under gravity. Depending on a number of factors such as the humidity in the lab and how freely the graphite is able to fall through the funnel, significant differences in the packing density could occur. Compounding this difficulty is the fact that the silicon insulation plugs used to confine the graphite to the central portion of the tubes are also packed into the tubes with varying amounts of force and, in addition, they vary in size somewhat. These two factors will create a back pressure that will be different from column to column causing the flow rates through each column to vary significantly. Coupled with the fact the flow rates are already very low to begin with, this may have resulted in samples not being exposed to the vapor long enough to reach equilibrium. Flow controllers cannot be used to measure the flow rate in each column since once the cesium vapor is introduced to the gas stream, the gas stream could be damaging to flow controllers of the type used in these experiments.

The packing of the graphite in the columns may also cause uneven exposure of the graphite samples to the cesium vapor. If the graphite packs under gravity in such a way that a portion of the column is less dense than the rest, the gas and vapor will flow more easily through this region and not expose surrounding

regions evenly. Mechanically packing the graphite into the column rather than letting it settle under gravity is unlikely to entirely mitigate this since it will still be difficult to pack the columns to exactly the same density.

It may be possible to improve upon this data by running the experiment for longer as this will reduce the effect of the differing flow rates. The problem of the packing densities will remain, however.

It is difficult to explain the over 9ppm result for the highest vapor concentration on the sample at 700°C. The simplest explanation is that the sample was somehow contaminated either during the experiment or (less likely), during analysis.

An additional problem not shown in the preceding data was the presence of strontium in the graphite samples. All the samples, including the blank sample that was never exposed to any part of the experimental system showed 4-5ppm of strontium present on them. Given that the amount of strontium contaminant was constant for all samples, it does not help to explain the inconsistency of the results but it certainly suggests the need for a different type of graphite.

Despite the inconsistencies in the data, there are some conclusions we can draw from them. Rejecting the anomalously high reading, it can be seen that for these vapor pressure, the concentration on any sample does not exceed 1ppm indicating that it will not be possible to detect mass changes during this adsorption process in the TGA. Again, rejecting the anomalously high reading, the average amount of cesium adsorbed across all concentration follows the

trend expected from past work. More vapor is adsorbed at lower temperatures, less as the temperature increases. Additionally, the data does seem to trend towards some maximum amount adsorbed as the vapor concentration increases. This amount appears to be somewhere between 700 and 900 ppb at 500°C and 600°C. Previous data suggests this saturation amount should be less at higher temperatures.

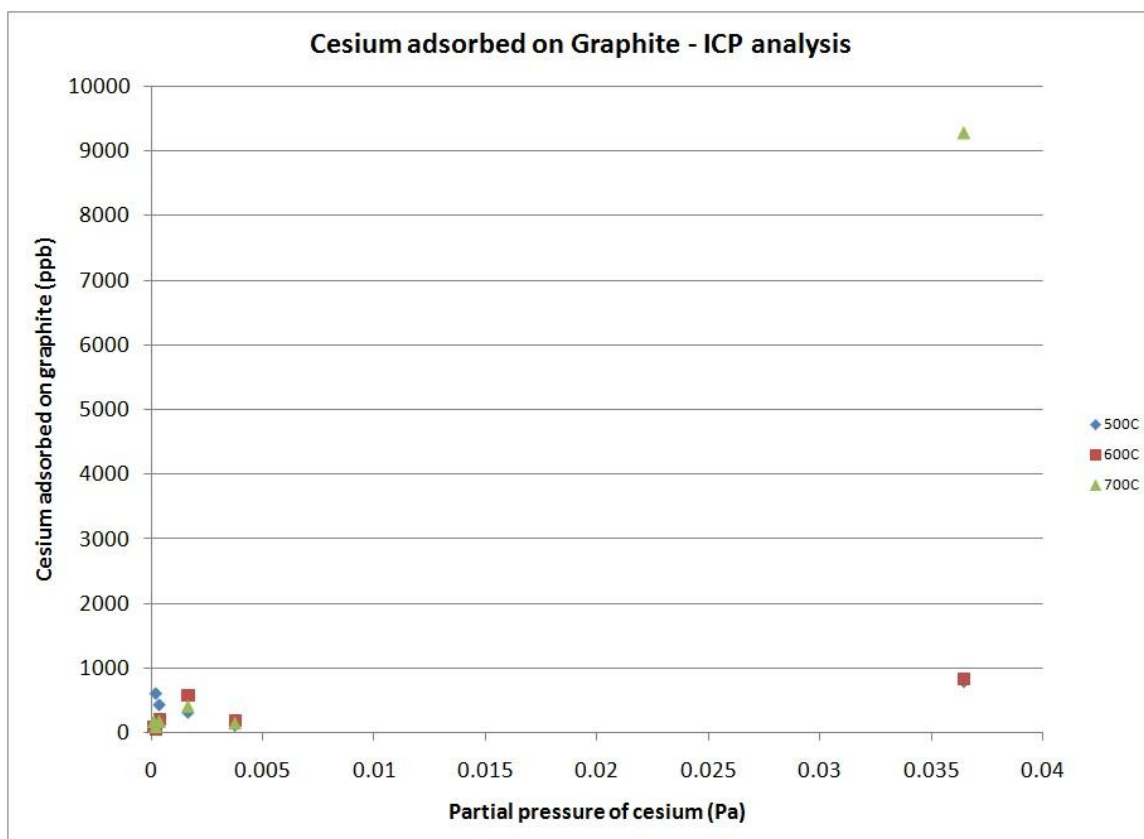


Figure 5.4.1 – Data from the ICP analysis of samples with cesium adsorbed on graphite

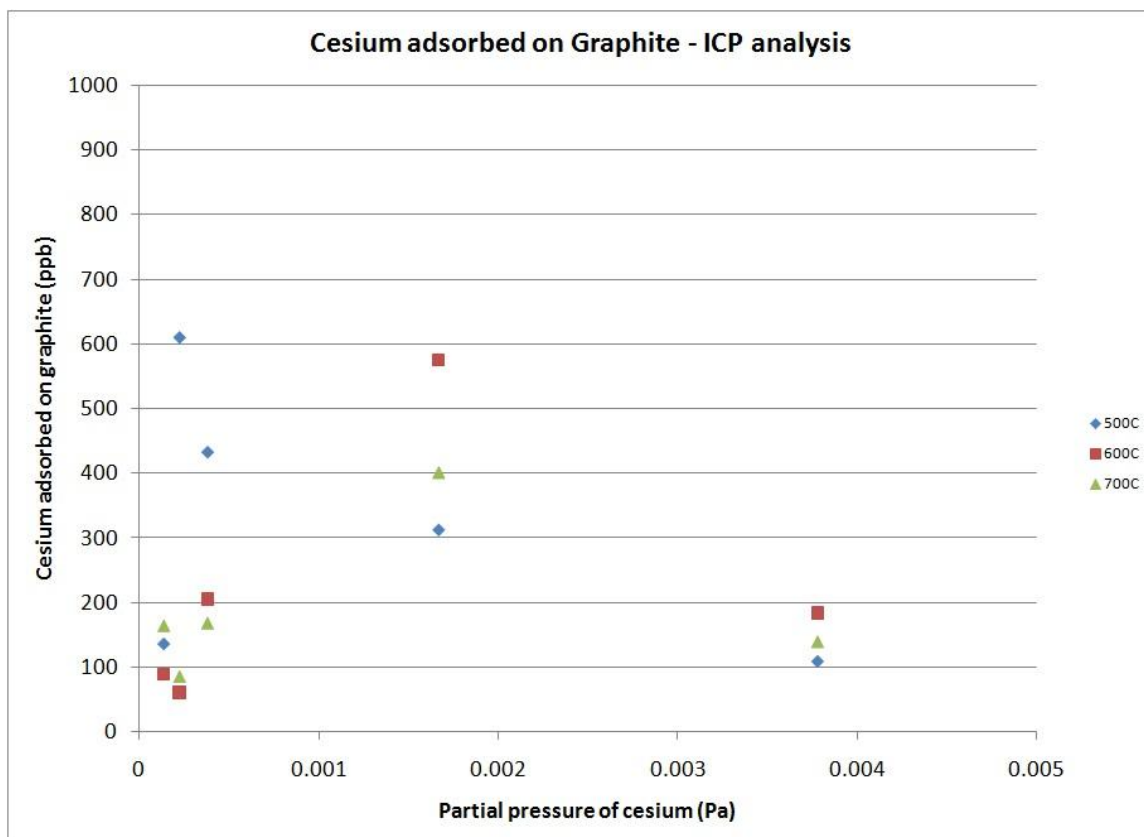


Figure 5.4.2 - Data from the ICP analysis of samples with cesium adsorbed on graphite with range closer to the origin

Chapter 6 - Conclusion

The adsorption of fission products on VHTR structural materials remains a subject of great importance in the design, certification and operation of these reactors. While we have made some progress in this work, a great deal more data is needed. Whatever the other deficiencies of this research program may be, the largest by far is simply that these studies have been conducted on commercially available graphite powder. Hilpert noted in 1985 that the adsorbed amount on different grades of graphite varies by orders of magnitude. Given this, the research program that we have conducted serves mainly as a study of the various methods we might use to make these measurements on modern reactor graphite.

Our results have shown that NAA and ICP are important and useful methods for making these measurements and each method is suited to some fission products, but not others. NAA is particularly useful for the measurement of iodine, and less useful for cesium. ICP has the opposite strengths and weaknesses. In general, it will not be possible to make these measurements gravimetrically. The adsorbed amounts are simply too low to detect in this manner.

The use of powdered graphite has proven to be problematic for reasons outlined in section 5.4. In the future, it may be preferable to design a sample of solid graphite with a flat, possibly polished surface that will allow vapor to flow over it. This will eliminate any of the possible packing problems associated with the use of powdered graphite and allow for a constant surface area of graphite to be exposed to the vapor. Such a sample might be an elongated cubical piece of graphite that could be placed inside a tube, either ceramic or a suitable metal alloy like inconel. If the sample was sufficiently long in relation to the tube, the flow over the longest exposed surface will be acceptably laminar and of constant rate. Once the sample run has ended, the elongated cube of graphite can be removed, the ends cut off (since the vapor impinging on the surface of the sample perpendicular to the gas flow will likely acquire a higher concentration of adsorbate, perhaps even due to condensation) and the long, top surface filed down with sand paper to a suitable depth and then collected and weighed. It will then be possible to characterize the amount adsorbed on this surface area and the depth profile of the adsorbate could also be measured by varying the depth of the filing. This hypothetical sample arrangement is shown in figure 6.1.

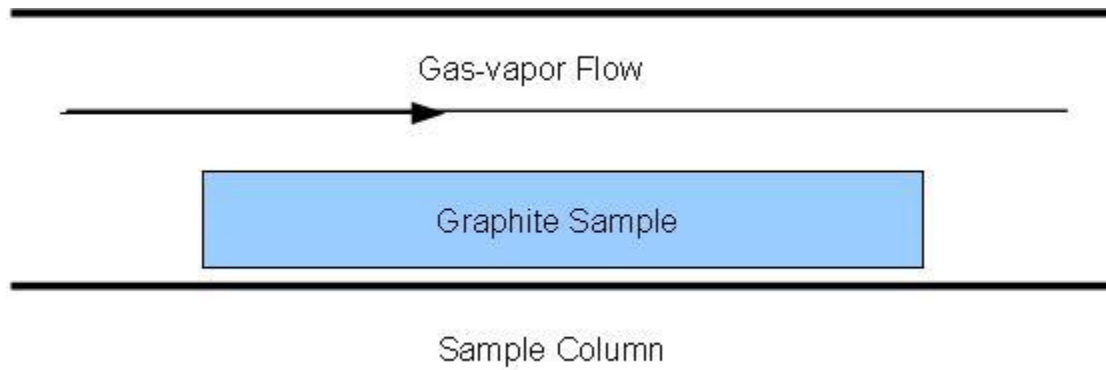


Figure 6.1 – Possible future graphite sample arrangement

The cell designed as part of this project for the production of cesium proved to be extremely helpful. Cesium is very dangerous to handle and this cell allows for its safe handling and use in a variety of experiments where we have a desire to produce cesium vapor. The use of this device or a similar one in any further experiments involving cesium is strongly recommended.

Splitting the gas laden vapor stream using the manifold that was part of this system is a viable method of running more than one sample at a time. If we depart from the use of graphite powder, it should merely be necessary to ensure the sample tubes are reasonably symmetric and that the experiment runs for sufficient time to allow for any possible difference in flow rates through the sample tubes.

Further experiments with less dangerous fission products can be conducted using a furnace tube to produce the vapor and NAA or ICP for the analysis of the resulting samples.

BIBLIOGRAPHY

1. J. P. STONE, C.T. EWING, J.R. SPANN, E.W. STEINKULLER, D.D. WILLIAM, and R.R. MILLER, High Temperature Vapor Pressures of Sodium, Potassium and Cesium, *Journal of Chemical and Engineering Data*, **Vol 11**, No3, 315 (1966).
2. J. B. TAYLOR, I. LANGMUIR, Vapor Pressure of Cesium by the Positive Ion Method, *Physical Review*, **Vol 51**, 753 (1937).
3. P. PRADEL, F. ROUSSEL and G. SPIESS, Measurements of the Vapor Pressure of Cesium by Absorption of Resonance Radiation, $\lambda = 8521 \text{ \AA}$, *Rev. Sci. Instrum.*, **Vol 45**, No1, 45 (1973).
4. G. I. GUSHCHIN, V. A. SUBBOTIN, E. KHACHATUROV, Saturated Vapor Pressure of Cesium in the 483-642 deg K range, *Teplofizika Vysokikh Temperatur*, **Vol 13**, No 4, 174 (1975).
5. E. E. SHPIL'RAIN, E. V. NIKANOROV, Cesium Vapor Pressure Studied by the Boiling Point Method, *Teplofizika Vysokikh Temperatur*, **Vol 10**, No 2, 297 (1972).
6. G. P. BAXTER, C. HICKEY and W. C. HOLMES, The Vapor Pressure of Iodine (2006).
7. M. BERKENBLIT and A. REISMAN, The Vapor Pressure of Iodine in the Temperature Interval 43-80C, *Journal of the Electrochemical Society*, **Vol 113**, No 1, 93, (1966).

8. W. RAMSAY, S. YOUNG, On the Vapour-pressures of Bromine and Iodine, *Journal of the Chemical Society*, **Vol 49**, 453 (1886).
9. H. ARCTOWSKI, Sublimation Tension of Iodine, *Zeitschrift fuer Anorganische Chemie*, **Vol 12**, 417 (1896).
10. A. WIEDERMANN, Vapor Pressure of some Solids, *Verhandl. Deut. Phys. Ges*, **Vol 7**, 159 (1905).
11. Yu. A. PRISELKOV, An. N. NESMEYANOV, Determination of the vapor pressures of calcium and strontium below their melting points by the method of tagged atoms. *Doklady Akademii Nauk SSSR*, **95** 1207-10 (1954).
12. A. J. H. BOERBOOM, et al. Heat of sublimation and vapor pressure of strontium. *Physica (The Hague)* **Vol 30**, 1, 254-7 (1964)
13. J. BOHDANSKY, H E. J. SCHINS, Vapor pressure of different metals in the pressure range of 50 to 4000 torr. *Journal of Physical Chemistry*, **Vol 71**, 2, 215-17 (1967)
14. R. OTTO; Hartmann, Hellmuth. Researches at high temperatures. XVII. The vapor pressures of the alkaline earth metals. *Zeitschrift fuer Anorganische und Allgemeine Chemie*, **Vol 133**, 29.45(1924)
15. M. ASANO and K. KUBO, Vapor Pressure of Strontium below 660K, *Journal of Nuclear Science and Technology*, **Vol 15**, 10, 765-767(1978)
16. J. W. ARBLASTER, Vapour Pressure Equations for the Platinum Group Elements, *Platinum Metals Rev*, **Vol 51**, 3, 130-135 (1995)

17. R. F. HAMPSON, and R. F. WALKER, The Vapor Pressure of Palladium, *Journal of Research of the National Bureau of Standards*, **Vol 66A**, 2, 177-178 (1961)
18. P. D. ZAVITSANOS, High-temperature vaporization studies using a recording micro-balance and electron-bombardment heating. I. Vapor pressure of silver. II. Vapor pressure of palladium. (1963)
19. M. B. PANISH, Vapor Pressure of Silver, *Journal of Chemical and Engineering Data*, **Vol 6**, 4, 592-594 (1961)
20. S. K. TARBY, and V. ROBINSON III, The Vapor Pressure of Liquid Silver, *Transactions of the Metallurgical Society*, **Vol 242**, 719-721 (1968)
21. I. ANSARA and E. BONNIER, Vapor pressure of Beryllium and Liquid Silver, *Conference internationale sur la metallurgie du beryllium* (1965)
22. L. A. HAAS and C. W. SCHULTZ, A Torsion Effusion Apparatus for Vapor Pressure Measurements – Vapor Pressure of Silver from 1200 to 1500K, *Bureau of Mines Report of Investigations*, 1965
23. Personal correspondence with Professor Viswanath
24. H. FREUNDLICH, Of the adsorption of gases – Section II – Kinetics and Energetics of Gas Adsorption, *Transactions of the Faraday Society*, 1932
25. I. LANGMUIR, A Theory of Adsorption, *Proceedings of the American Physical Society*, **Vol VI**, 1, 79-80 (1915)
26. S. BRUNAUER, P. H. EMMETT, and E. TELLER, Adsorption of Gases in Multimolecular layers, *J. Am. Chem. Soc.*, **60** (2), pp 309–319., (1938)

27. A. YOUNG and D. CROWELL, Physical Adsorption of gases, (1962)
28. B.F. MYERS, W.E. BELL, Cesium Transport Data for HTR Systems, GA-A13990, General Atomic, 1979
29. B.L. HOLIAN, The Interaction between Cesium and Graphite for use in the Study of Surface Phenomena, *Nuclear Metallurgy*, **20**, (1976)
30. Z.P. HU, N.J. WU and A. IGNATIEV, Cesium adsorption on graphite (0001) surface: The phase diagram, *Physical Review B*, **33**, 11, (1985)
31. M.E. PHILLIPS, Modeling of Caesium deposition in CAGR Reactor Circuits
32. R. REPANSZKI, Z. KERNER and G. NAGY, Adsorption of fission products on stainless steel and zirconium, *Adsorption*, **13**, 201-207, (2007)
33. T. SEYLLER, R. HASENEDER, E. REINHART, D. BORGMANN, G. WEDLER, Characterization of K and Cs adsorption on Fe(110), *Surface Science*, **424**, (1999)
34. K. HILPERT, H. GERADS, D. KATH, D. KOBERTZ, Sorption of cesium and its vaporization from graphitic materials at high temperatures, *High Temperatures – High pressures*, **20**, 157-164 (1988)
35. K. IWAMOTO and J. OISHI, The Behavior of Iodine in Adsorption and Desorption by Graphite, *Journal of Nuclear Science and Technology*, **5**, 9, (1968)
36. M. V. OSBORNE, R. B. BRIGGS, Iodine Adsorption on Steel in Helium, *Transactions of the American Nuclear Society*, (1979)

37. K HILPERT, H GERADS, D KOBERTZ, Sorption of Strontium by Graphitic Materials, *Berichte der Bunsengesellschaft für physikalische Chemie*,(1984)
38. B.F. MYERS, W.E. BELL, Strontium Transport Data for HTR Systems, GA-A--13168, General Atomic, 1974
39. IAEA TECDOC 976, Fuel performance and fission product behavior in gas cooled reactors, 1997

VITA

Sean Branney was born near Castlewellan, Northern Ireland on May 31st, 1980. He attended Queens University, Belfast earning a B.S. in physics in July of 2001 and acquiring a black belt in World Ju-Jitsu Federation Ju-Jitsu along the way. He moved to the United States in July of 2002 and returned to education at the University of Missouri, Columbia where he received an M.S. in Nuclear Engineering with an emphasis in power in July 2008, one month after being naturalized as a U.S citizen at a ceremony in Kansas City, Missouri. Sean remained at the University of Missouri, Columbia to complete his Ph.D in Nuclear Engineering, this thesis being the culmination of that work. Sean is also a nationally ranked powerlifter with a best competition total of 1251lbs at the American Drug Free Powerlifting Federation National championships in June 2010.